Early to Late Maastrichtian Environmental Changes in the Indian Ocean Compared with Tethys and South Atlantic

Paula Mateo[1*], Gerta Keller[1], Jahnavi Punekar[1] and Jorge E. Spangenberg[2]

[1]Department of Geosciences, Princeton University, Princeton, New Jersey 08544, USA

[2]Institute of Earth Surface Dynamics, University of Lausanne, Lausanne 1015, Switzerland

[*]Corresponding author: mmateo@princeton.edu (email address); Guyot Hall, Princeton University, Princeton, New Jersey 08544, USA (mailing address); +1(609)-917-4895 (phone number)

ABSTRACT: Planktic foraminiferal analysis, including species populations, diversity trends, high-stress indices and stable isotopes of the latest Campanian through Maastrichtian in the South Atlantic, Tethys and Indian oceans reveal four major climate and faunal events that ended with the Cretaceous-Paleogene (K/Pg), formerly Cretaceous-Tertiary (K/T), mass extinction. The prelude to these events is the late Campanian cooling that reached minimum temperatures in the earliest Maastrichtian (base C31r) correlative with low primary productivity and species diversity. Event-1 begins during the persistent cool climate of the early Maastrichtian (lower C31r) when primary productivity rapidly increased accompanied by rapid species originations,

attributed to increased nutrient influx from increased upwelling, erosion during the sea-level fall ~70.6 Ma, and Ninety East Ridge volcanism. During Event-2 (upper C31r to lower C30n), climate rapidly warmed by 2-3 °C in deep waters and peaked at 22 °C on land, primary productivity remained high and diversification reached maximum for the entire Cretaceous. We attribute this climate warming to intense Ninety East Ridge volcanic activity beginning ~69.5 Ma, accompanied by rapid reorganization of intermediate oceanic circulation. Enhanced greenhouse conditions due to the eruption of Deccan Phase-1 in India resulted in detrimental conditions for planktic foraminifera marking the end of diversification. Global cooling resumed in Event-3 (C30n), species diversity declined gradually accompanied by dwarfing, decreased large specialized species, increased small ecologically tolerant taxa, and ocean acidification. Event-3 is mainly the result of enhanced weathering and volcanogenic CO_2 adsorption by the oceans during the preceding warm Event-2 that led to cooling and lower pH in the surface ocean. Event-4 marks the last 250 kyr of the Maastrichtian (C29r), which began with the largest Deccan eruptions (Phase-2) that caused rapid climate warming of 4 °C in deep waters and 8 °C on land, acid rain and ocean acidification leading to a major carbonate crisis preceding the K/T mass extinction.

1 INTRODUCTION

The Maastrichtian (the last stage of the Late Cretaceous, 72.1-66.0 Ma; Gradstein et al., 2012) is a 6.1-Myr time interval that experienced climate and biological extremes ranging from maximum cooling to maximum warming and from maximum marine evolutionary diversity to one of the largest mass extinctions in Earth's history at the Cretaceous/Tertiary (K/T; also known as Cretaceous-Paleogene K/Pg) boundary (review in Keller et al., 2016a).

Despite this remarkable 6.1-Myr history of environmental changes, the Maastrichtian is mostly known for the mass extinction. For the past 30 years, research has concentrated on the K/T boundary centering on a contentious debate: was the mass extinction instantaneous and caused by an asteroid impact or was it more gradual and the result of long-term environmental changes with the asteroid impact the final coup de grace? There are multiple lines of evidence that unquestionably support an impact on the Yucatan Peninsula, Mexico: 1) the global iridium anomaly at the K/T boundary (Alvarez et al., 1980, Alvarez, 1983) that has become the hallmark for all K/T mass extinction studies, 2) discovery of the impact crater on Yucatan (Hildebrand et al., 1991), 3) global distribution of shocked quartz (e.g., Izett, 1990), 4) impact glass spherules discovered throughout the region surrounding the Chicxulub crater (e.g., Smit et al., 1992, 1996; Smit, 1999; Rocchia et al., 1996; Olsson et al., 1997; Norris et al., 1999; MacLeod et al., 2007; Schulte et al., 2010; Keller et al., 2013), and 5) impact breccia in the Chicxulub crater and large

55 breccia and conglomerate deposits lacking impact glass but interpreted as generated by seismic
56 disturbance from the Chicxulub impact (e.g., Bralower et al., 1998; Arenillas et al., 2006;
57 Schulte et al., 2010). Likely environmental consequences of the Chicxulub impact have been
58 widely discussed (e.g., Schultz and D'Hondt, 1996; Tsujita, 2001; Kring, 2007; Vellekoop et al.,
59 2014). This is a formidable list of characteristics that unquestionably identify an impact on
60 Yucatan, but did this impact crash into Yucatan precisely at K/T time and cause the mass
61 extinction as widely inferred? There is stratigraphic, geochemical, sedimentary and fossil
62 evidence that indicates this impact predates the mass extinction by about 100 kyr (Keller, 2014,
63 and references therein). This is a key issue in this ongoing debate over the cause of the K/T mass
64 extinction.

65 Various advances over the past 10 years have shown that Deccan Trap volcanism in India
66 could have been a critical source of environmental stress leading to the K/T mass extinction: (1)
67 Deccan eruptions were most intense during magnetochron C29r spanning the K/T boundary
68 (Chenet et al., 2007, 2008, 2009); (2) high-precision age based on U-Pb geochronology revealed
69 that 80 % of Deccan eruptions occurred over the ~750 kyr (duration of C29r) with accelerating
70 intensity across the K/T boundary (Schoene et al., 2015); (3) documentation of the mass
71 extinction in intertrappean sediments in India (Keller et al., 2011) between the longest lava flows
72 recorded on Earth (Self et al., 2008); (4) rapid climate warming during C29r below the K/T

boundary due to large inputs of volcanogenic greenhouse gases (reviews in Punekar et al., 2014a; Keller et al, 2016a). Based on these studies, it was suggested that the Chicxulub impact might have accelerated Deccan volcanism leading to the mass extinction (Richards et al., 2015; Renne et al., 2015). With this changing perspective, a better understanding of the preceding Maastrichtian environmental changes is imperative and the focus of this study.

One of the first detailed studies on Campanian to early Maastrichtian climate is from Shatsky Rise, Pacific Ocean: stable isotope records based on planktic and benthic foraminifera revealed ~2.5 °C and ~4 °C cooling in surface and bottom waters, respectively (Douglas and Savin, 1975). Subsequent studies on Seymour Island, Antarctica, and ODP Site 690 in the Weddell Sea reported ~2 °C cooling in surface and bottom waters during the early Maastrichtian (Barrera et al., 1987; Barrera and Huber, 1990; Barrera, 1994). The first high-resolution study of Maastrichtian climate and associated faunal turnovers in planktic foraminifera was based on South Atlantic DSDP Site 525A (Li and Keller, 1998a, b; Abramovich and Keller, 2003). These studies revealed that the generally cool Maastrichtian climate was interrupted by two rapid warm events: 1) at the early to late Maastrichtian transition (also known as mid-Maastrichtian event) with a 2-3 °C warming of surface and bottom waters, and 2) in the latest Maastrichtian below the K/T boundary (C29r) when surface and bottom waters warmed rapidly by 4 °C. An updated high-resolution stable isotope record for the late Campanian to early Maastrichtian at Site 525A

confirmed the observed cooling and warming events (Friedrich et al., 2009). Since Li and Keller (1998a, b), the latest Maastrichtian C29r rapid marine warming has been documented globally (e.g., Barrera and Savin, 1999; MacLeod et al., 2005; Isaza-Londoño et al., 2006; Tobin et al., 2012; Thibault and Husson, 2016) and recently linked to the main phase of Deccan volcanism (reviews in Punekar et al., 2014a; Keller et al, 2016a). Some studies correlate the Maastrichtian terrestrial and marine climate records demonstrating that the same extreme climate changes occurred also on land (Nordt et al., 2003; Wilf et al., 2003).

In addition to the climate record, various studies focused on Maastrichtian primary productivity, sea-level fluctuations and the marine biotic response to climate changes based on planktic foraminifera (e.g., Li and Keller 1998a, c; Zepeda, 1998; Premoli Silva and Sliter, 1999; Li et al., 2000; MacLeod et al., 2001; Olsson et al., 2001; Abramovich and Keller, 2002, 2003; Abramovich et al., 2003, 2010; Hart, 2007; Punekar et al., 2014b) and nannofossils (e.g., Eshet and Almogi-Labin, 1996; Friedrich et al., 2005; Thibault and Gardin, 2007, 2010; Gardin et al., 2012; Thibault, 2016; Thibault and Husson, 2016). A particular focus of these studies is the early to late Maastrichtian warming and associated minor extinctions (review in Keller et al., 2016a) as well as the rapid warming during C29r and associated diversity decline (review in Punekar et al., 2014a).

The eruption of Large Igneous Provinces (LIPs) have been shown to be a direct cause for climate change (both cooling and warming), acid rains, ocean acidification and large inputs of toxic metals, as well as an indirect cause for anoxia and changes in sea-level and oceanic circulation disruptions, leading to major faunal turnovers including mass extinctions (e.g., Siberian Traps and Permo-Triassic, Central Atlantic (CAMP) and the Triassic-Jurassic, Deccan Traps and Cretaceous-Tertiary) (Wignall, 2001; Courtillot and Renne, 2003; Bond and Wignall, 2014; Courtillot and Fluteau, 2014). During the Maastrichtian, Ninety East Ridge volcanism in the Indian Ocean was active (e.g., Duncan, 1978, 1991; Pringle et al., 2008; Krishna et al., 2012) and overlapped the eruption of Deccan phase-1 in India (Chenet et al., 2009; Schöbel et al., 2014) potentially contributing to the climate and faunal changes recorded during this time.

The main objective of this study is to evaluate the environmental effects of climate change and major volcanic eruptions on marine planktic foraminifer diversity during the Maastrichtian. We test the hypothesis that volcanism was the main driver of the evolutionary diversification in the early Maastrichtian, the likely cause for the early to late Maastrichtian climate warming, and the latest Maastrichtian warming (C29r) and high-stress environments. We focus on five localities from the Indian Ocean (Ninety East Ridge Site 217, Cauvery Basin, SE India), Tethys (El Kef and Elles, Tunisia) and South Atlantic (Site 525A) (Fig. 1). Analyses concentrate on: 1) high-resolution quantitative analysis of planktic foraminifera to determine

biostratigraphy and assess the timing and nature of faunal turnovers at Site 217; 2) update taxonomy of the Tethys and South Atlantic sites, and extend the Cauvery Basin record through the early Maastrichtian to compare diversity trends through the Maastrichtian; 3) oxygen and carbon stable isotopes of planktic and benthic foraminifera at Site 217 to evaluate changes in climate and productivity compared with Site 525A; 4) planktic foraminiferal indices, including diversity, dwarfing, planktic/benthic ratio and fragmentation index, to gain a deeper understanding of the changing environment and associated faunal responses; and 5) correlation of sedimentation records, hiatus distribution and sea-level changes across regions Indian, Tethys and South Atlantic oceans to understand regional and global effects of climate and ocean circulation changes.

2 MATERIALS AND METHODS

DSDP Site 217 (8°55.57'N, 90°32.33'E) is located in the Indian Ocean on the northernmost part of the Ninety East Ridge at a water depth of 3010 m (Von der Borch et al., 1974). Ninety East Ridge is interpreted as a volcanic chain formed by the northward migration of the Indian plate over the Kerguelen mantle plume that was active from the late Cretaceous to the Paleogene (e.g., Duncan, 1978, 1991; Pringle et al., 2008; Krishna et al., 2012). With the passage

144 over the mantle plume, lithospheric uplift led to the formation of volcanic islands and the
145 deposition of thick ash sequences and shallow water sediments overlying the basement (Moore et
146 al., 1974; Thompson et al., 1974; Coffin, 1992); passage beyond the mantle plume led to rapid
147 subsidence as the oceanic lithosphere cooled (Sclater and Fisher, 1974; Luyendyk, 1977; Coffin,
148 1992). Based on a linear progression rate of 118 km/Myr, an age of ~80 Ma was estimated for
149 the location of Site 217 at the time of its position over the mantle plume (Pringle et al., 2008),
150 which is consistent with the Campanian age of the oldest sediments recovered with shallow
151 water affinities overlying the basement (Von der Borch et al., 1974). A progressive deepening to
152 a depth of ~1000 m is recorded during the early to late Maastrichtian as indicated by the
153 transition to foraminifera-rich nannofossil ooze (Von der Borch et al., 1974; Tantawy et al.,
154 2009).

155 Samples were taken every ~50 cm from cores 17 to 21; planktic foraminifera were
156 originally analyzed by Alfonso Pardo and published in Tantawy et al. (2009). For this study, the
157 species identifications were updated and additional size fractions were analyzed to focus on the
158 very small (38-63 μm), small (63-150 μm) and larger (>150 μm) size fractions as environmental
159 indicators. In addition, sample resolution was increased and additional samples were added to
160 extend the record through core 23. A total of 70 samples were analyzed.

For paleontological analyses, samples were processed in the laboratory following the procedure described by Keller et al. (2002). Samples were soaked overnight in 3 % hydrogen peroxide solution to oxidize organic carbon. After disaggregation of sediment particles, the samples were washed through >63 μm and >38 μm sieves to obtain clean foraminiferal residues. Washed residues were oven dried at 50 °C. Quantitative planktic species analyses were performed based on aliquots of 300 specimens in the 38–63 μm, 63-150 μm and >150 μm size fractions, with the remaining residues in each sample fraction examined for rare species. All specimens were identified based on standard taxonomic concepts (Robaszynski et al., 1983-1984; Nederbragt, 1991) and mounted on microslides for a permanent record.

Oxygen and carbon isotope analyses were performed on monospecific benthic foraminiferal tests (*Gavelinella beccariformis* and *Cibicidoides* species) in laboratories at Karlsruhe University, Germany, and at the University of Lausanne, Switzerland. At the Karlsruhe laboratory, the data were obtained using a fully automated preparation system (MultiCarb) connected on-line to an isotope ratio mass spectrometer (Optima, Micromass Limited UK). All carbon and oxygen isotope values are reported relative to the VPDB standard, with reproducibility better than 0.1 ‰ (2σ). At the UNIL laboratory, analyses were performed for cores 21-23 with a Thermo Fisher Scientific (Bremen, Germany) GasBench II connected to a Thermo Fisher Scientific Delta Plus XL IRMS, in continuous He-flow mode. Analytical

uncertainty (2σ) monitored by replicate analyses of the international calcite standard NBS-19 ($\delta^{13}C$ = +1.95 ‰, $\delta^{18}O$ = −2.20 ‰) and the laboratory standard Carrara Marble ($\delta^{13}C$ = +2.05 ‰, $\delta^{18}O$ = −1.70 ‰) was better than ± 0.05 ‰ for $\delta^{13}C$ and ± 0.1 ‰ for $\delta^{18}O$. Results from both laboratories are comparable based on replicate analyses.

Species diversity was estimated based on cumulative species richness: number of species theoretically present in any given sample from first evolutionary appearance to extinction, ignoring any temporary exclusion (Abramovich and Keller, 2002). Species dwarfing estimates were based on the number of 150-250 μm specimens in the >150 μm size fraction of each sample. The planktic/benthic foraminiferal ratio was based on the number of benthic foraminifera associated with the aliquot of 300 planktic foraminifera used for the quantitative species analysis in the 63-150 μm size fraction.

The fragmentation index (FM) was analyzed based on aliquots of approximately 500-700 foraminifera and fragments in the >63 μm size fraction. Three categories were identified based on the quality of preservation: 1) nearly perfect tests (good), 2) partially damaged, imperfect tests with holes (fair), and 3) fragments, less than two-thirds of an entire test (poor) (Punekar et al., 2016). The FM index was calculated as $fragments\% = (fragments/8)/[(fragments/8) + whole\ tests]$ (Williams et al., 1985; Malmgren, 1987). Based on the assumption that each test

196 breaks into an average of 8 fragments, the equation requires the total number of counted
197 fragments to be divided by 8 to estimate the original number of whole tests.

198 At the Cauvery Basin, India, we chose the Kali-H subsurface core previously analyzed in
199 Keller et al. (2016b) for the upper Maastrichtian and extended this record through the lower
200 Maastrichtian concentrating on species diversity and ranges from first to last appearances. To
201 insure that the same species concepts were used in faunal analyses, species identifications were
202 updated for the Tunisian sections in Elles and El Kef (Li and Keller, 1998c; Abramovich and
203 Keller, 2002) and South Atlantic DSDP Site 525A (Li and Keller, 1998a).

204

205 **3 BIOSTRATIGRAPHY**

206

207 **3.1 Ninety East Ridge DSDP Site 217, Indian Ocean**

208

209 High-resolution planktic foraminiferal biostratigraphy is a powerful tool for relative age
210 dating and to assess the continuity of sediment deposition. In this study, we apply the Cretaceous
211 foraminiferal (CF) biozonation of Li and Keller (1998a) and correlate the results with localities
212 from the Indian, Tethys and South Atlantic oceans (Fig. 2).

213 The Maastrichtian interval at DSDP Site 217 spans zones CF8 to CF2 and was analyzed
214 in two size fractions, >150 μm to evaluate relative abundances of larger specialized species and
215 63-150 μm to evaluate the smaller ecological generalist taxa.

216 Zone CF8 is defined by the first appearance (FA) of *Globotruncana aegyptiaca* at the
217 base and the FA of *Gansserina gansseri* at the top (Fig. 2). At Site 217, a 5 m core gap prevents
218 full assessment of zone CF8 and only the upper part may be present, assuming that the first
219 appearance of *G. aegyptiaca* occurs below the analyzed interval (Fig. 3). Nine species appear
220 above the core gap based on both size fractions (>150 μm, 63-150 μm). These species
221 originations are part of the gradual diversification event that began in zone CF8 and was
222 previously observed at Elles and El Kef, Tunisia, and South Atlantic DSDP Site 525A (Li and
223 Keller, 1998a, c).

224 Zone CF7 spans the interval between the FA of *G. gansseri* at the base and the FA of
225 *Contusotruncana contusa* at the top (Fig. 2). At Site 217, a gradual increase in the relative
226 abundance of *Gublerina rajagopalani* from 6.5 % to 16 % is observed in the >150 μm size
227 fraction (Fig. 3) and in *Heterohelix planata* from 23 % to 45 % in the 63-150 μm size fraction
228 (Fig. 4). These species have been shown to tolerate and thrive in a wide range of environmental
229 conditions (i.e., dominant in high-stress environments affected by temperature, salinity, nutrients
230 and oxygen variations in which large specialized species struggle to survive), thus their

231 increasing population abundances suggest increasing stressed environments (e.g., Pardo and
232 Keller, 2008; Keller and Abramovich, 2009).

233 Zone CF6 is defined by the FA of *C. contusa* at the base and the last appearance (LA) of
234 *Globotruncana linneiana* at the top. The latter species also marks the base of zone CF5 and the
235 FA of *Racemiguembelina fructicosa* defines the top (Fig. 2). At Site 217, zone CF6 is at least
236 partially present, but zone CF5 is not recognized due to a core gap and likely hiatus as just ~2 m
237 of sediments represent the combined CF6-CF5 interval (Figs. 3, 4). In contrast, these two zones
238 span 8 m and 5 m in the Cauvery Basin of SE India (Keller et al., 2016b), 6.5 m and 9.5 m at
239 South Atlantic Site 525A, (Li and Keller, 1998a), 4 m and 13 m at El Kef, and 4.5 m and 6.5 m
240 at Elles, Tunisia (Li and Keller, 1998c), respectively. However, at Site 525A and the Tunisian
241 sections, zone CF6 is condensed (~5 m) suggesting widespread erosion between CF5 and CF6,
242 coincident with a sea-level fall and major sequence boundary (SB) dated at 69.4 Ma (Fig. 2)
243 (Haq et al., 1987; Haq, 2014).

244 Zone CF4 spans the interval from the FA of *R. fructicosa* at the base to the FA of
245 *Pseudoguembelina hariaensis* at the top (Fig. 2). At Site 217, a minor extinction event is marked
246 by the disappearances of *Contusotruncana fornicata*, *C. plummerae* and *Globotruncana*
247 *bulloides* (Fig. 3). These species disappearances, frequently including *Archeoglobigerina*
248 *cretacea*, have also been recognized at Site 525A, Madagascar, Israel, Egypt, Tunisia, Poland

and SE India (Li and Keller, 1998a, c; Abramovich et al., 1998, 2002, 2010; Dubicka and Peryt, 2012; Meilijson et al., 2014; Punekar et al., 2014b; Keller et al., 2016b). Zone CF4 is marked by decreased abundance of *Rugoglobigerina rotundata* from 10 % to 3 % and *R. rugosa* from 5 % to 2 %, and increased abundance of *G. rajagopalani* from 10 % to 43.5 % followed by a rapid decrease to 20 % towards the top of CF4 (Fig. 3). In the smaller size fraction (63-150 μm), major species variations include decreased abundance of *H. planata* parallel to increased abundances of *Globigerinelloides yaucoensis* from 19 % to 54.5 % and *G. asper* from 14 % to 36 %, reaching minimum values at the CF4/CF3 boundary (Fig. 4).

The CF4/CF3 boundary is marked by a hiatus as suggested by the abrupt decrease in all larger (>150 μm) species abundances (Fig. 3) and increase in very small stress-tolerant species (e.g., globigerinellids, globotruncanellids, hedbergellids, guembelitrids, Fig. 4). A hiatus at the CF4/CF3 transition coincides with a major sea-level fall and SB ~66.8 Ma (Haq et al., 1987; Haq, 2014) and is recorded worldwide (e.g., SE India, Keller et al., 2016b; Madagascar, Abramovich et al., 2002; Israel, Abramovich et al., 1998; Fig. 2).

Zone CF3 is defined by the FA of *P. hariaensis* at the base and the LA of *G. gansseri* at the top (Fig. 2). At Site 217, *G. rajagopalani* and *Pseudoguembelina palpebra* dominate and *Abathomphalus mayaroensis* is common in the >150 μm size fraction of zone CF3 assemblages (Fig 3). Dwarfed specimens are common in several horizons (424.08 m, 424.59 m, 425.19 m,

426.70 m, 432.96 m, and 441.58 m). In the smaller size fraction (63-150 μm) *Heterohelix*, *Globigerinelloides*, and *Globotruncanella* (*havanensis*, *petaloidea*) species dominate (Fig. 4). The disaster opportunist *Guembelitria cretacea* records increased abundances from 1 % to 5 % on average. These faunal changes indicate continued and even increasing high-stress environments during zone CF3 compared with zone CF4 (e.g., Pardo and Keller, 2008; Keller and Abramovich, 2009).

The CF3/CF2 transition is represented by a hiatus marked by abrupt changes in the relative abundances of larger species (Fig. 3) and smaller species (Fig. 4). This hiatus coincides with a sea-level fall ~66.25 Ma (Haq et al., 1987; Haq, 2014) and is commonly observed in the Indian and Tethys Oceans (e.g., Abramovich et al., 1998, 2002; Keller, 2005; Tantawy et al., 2009; Punekar et al., 2014b; Fig. 2).

Zone CF2 spans the interval from the LA of *G. gansseri* at the base to the FA of *Plummerita hantkeninoides* at the top (Fig. 2). At Site 217, this zone is marked by decreased abundance of *Gublerina rajagopalani* from 27 % to 10 % and increased *Pseudoguembelina palpebra* from 12 % to 20 % in the >150 μm size fraction (Fig. 3). In the 63-150 μm size fraction, small species abruptly increase (e.g., *Heterohelix*, *Globigerinella*, *Globotruncanella*, *Hedbergella*). *Pseudoguembelina costulata*, a surface dweller, dominates both the larger and the smaller size fractions towards the top of the section, with peak abundances of 31 % and 20 %,

respectively. This change is accompanied by a rapid increase in the abundance of *Guembelitria* species in the 38-63 μm size fraction suggesting severe high-stress environments just before the KTB hiatus (Fig. 4).

At Site 217, a major hiatus (~2 Myr) spans from the upper part of zone CF2 through the latest Maastrichtian zone CF1 and early Danian zones P0, P1a, P1b and lower P1c (Fig. 2). On a global basis, erosion is less extensive in this interval but marked by repeated short hiatuses. This erosion pattern is commonly attributed to rapid climate changes, periods of global cooling, intensified bottom-water circulation, and sea-level fluctuations across the K/T transition (e.g., MacLeod and Keller, 1991; Keller et al., 2013; Mateo et al., 2016).

3.2 Correlation: Indian, Tethys and South Atlantic Oceans

Biostratigraphic correlation of localities across the Indian, Tethys and South Atlantic oceans compared with major sea-level changes and volcanic eruptions in India (Deccan Traps) and Ninety East Ridge reveal similarities and differences in sedimentation related to these events (Fig. 2). Although the current study concentrates on the Maastrichtian, the early Paleocene (Danian) record is also shown as it illustrates the pivotal change in sediment deposition and erosion pattern that began in the late Maastrichtian zone CF3.

303 The early Maastrichtian sediment record across the regions is remarkably continuous
304 despite major sea-level fluctuations, Ninety East Ridge volcanic eruptions and associated climate
305 changes (Fig. 2). The only significant interruption coincides with the sea-level fall and sequence
306 boundary (SB) at ~69.4 Ma (Haq, 2014) correlative with zone CF5. The likely reasons for the
307 reduced sediment erosion include lower magnitude of sea-level changes, overall higher
308 Cretaceous oceans inundating continents, higher rate of carbonate sedimentation and relatively
309 low levels of volcanic eruptions.
310 In contrast, sedimentation is highly fragmented during the latest Maastrichtian beginning
311 in zone CF3 and continuing through the early Danian, except for areas protected from erosion,
312 particularly in Tunisia (Fig. 2). Sediment erosion (hiatus) generally coincides with sea-level
313 changes in zones CF4/CF3, CF3/CF2, KTB, P1a/P1b, P1b/P1c and P1c/P2. On Ninety East
314 Ridge, Southeast India (Cauvery Basin), Madagascar and South Atlantic, erosion removed
315 sediments spanning most of the early Danian and frequently through the KTB and zones CF1-
316 CF2. This massive erosion is also observed in the North Atlantic (Keller et al., 2013; Mateo et al.,
317 2016) and appears related to the significant sea-level fall at ~63.8 Ma, but a series of smaller sea-
318 level falls contributed to erosion that resulted in shorter hiatuses observed in the Tethys (e.g.,
319 Israel, Egypt) and many deep-sea sections. However, the major erosion observed during the
320 latest Maastrichtian through Danian can be attributed to the overall cooler climate (except for the

short warming in C29r), lower sea-level and higher frequency of sea-level falls beginning in CF3 (C30n).

4 STABLE ISOTOPES: PRODUCTIVITY AND TEMPERATURE CHANGES

Carbon and oxygen isotopes of the benthic foraminifera *Gavelinella beccariformis* were analyzed for the Maastrichtian at Site 217, except for zone CF8 where this species is rare and *Cibicidoides* species were analyzed instead. Both of these species are commonly used to evaluate deep-water changes in productivity and temperature (e.g., Shackleton 1987; Zachos et al., 1989; Schrag et al., 1995; D'Hondt and Arthur, 2002). Although Site 217 has a fragmented record because of frequent core gaps, $\delta^{13}C$ and $\delta^{18}O$ trends are similar to Site 525A (Li and Keller, 1998a), except for zones CF8-CF7. At Site 217, $\delta^{13}C$ values are significantly higher in CF8 (+1.46 ‰) and fluctuating in CF7 (+0.90 to +1.93 ‰) compared to Site 525A (+0.33 ‰ and +0.50 to +1.17 ‰, respectively) (Fig. 5). At Site 525A, $\delta^{13}C$ values record an increase of +1.5 ‰ through the early Maastrichtian that is not observed at Site 217 (Fig. 5). This difference likely reflects higher, more stable primary productivity at Site 217 due to higher nutrient inputs from Ninety East Ridge volcanism that began ~82 Ma (Coffin et al., 2002). Species effects are another

potential contributing factor to this difference because *G. beccariformis* at Site 217 is compared with *Anomalinoides acuta* at Site 525A (e.g., Friedrich et al., 2006).

At Site 217, the CF6-CF5 interval is incomplete due to a core gap and possibly a hiatus. In zone CF4, $\delta^{13}C$ values range from +1.1 ‰ to +1.6 ‰ similar to Site 525A (+1.2 ‰ to +1.7 ‰), suggesting sustained high primary productivity at both sites (Fig. 5). $\delta^{18}O$ values increase from +0.1 ‰ to +0.7 ‰ towards the top of zone CF4 at Site 217 marking cooling also comparable to Site 525A where $\delta^{18}O$ values increase from +0.1 ‰ to +0.5 ‰ (Fig. 5). In zones CF3-CF2, Site 217 $\delta^{13}C$ values vary from +0.9 ‰ to +1.7 ‰ similar to Site 525A (+1.2 to +1.8 ‰); in zone CF2, Site 217 $\delta^{18}O$ values decrease from +0.3 ‰ to −0.5 ‰, also comparable to Site 525A (+0.4 ‰ to −0.3 ‰), indicating climate warming.

5 DIVERSITY TRENDS

Planktic foraminifera are characterized by major evolutionary diversification in the early Maastrichtian and the mass extinction at the K/T boundary (review in Li and Keller, 1998a). The cause for this diversification event has remained an enigma and its potential contribution to the mass extinction is rarely considered. We use species ranges and cumulative species richness in the Indian, Tethys and South Atlantic oceans to investigate the early Maastrichtian origination

356 event and the fate of the new species leading up to the mass extinction. In the Indian Ocean
357 Ninety East Ridge Site 217 (Fig. 6) and the Kali-H well from the Cauvery Basin, SE India (Fig.
358 7), sediment deposition and faunal changes occurred at depths of 500-1000 m (upper to middle
359 bathyal; Von der Borch et al., 1974; Tantawy et al., 2009) and 300-500 m (outer shelf to upper
360 bathyal; Keller et al., 2016b), respectively. The El Kef and Elles sections in Tunisia (Fig. 8) were
361 deposited in outer shelf to upper slope (300-500 m) and middle to outer shelf (200-300 m) depths,
362 respectively. These are the two most complete Maastrichtian sedimentary records known
363 worldwide (Fig. 2) (Li and Keller, 1998c; Abramovich and Keller, 2002). In the South Atlantic,
364 Site 525A (Fig. 9) sediment deposition during the Maastrichtian occurred in a middle bathyal
365 environment (~1000 m) (Li and Keller, 1998a). The paleodepth of these five localities thus yield
366 comparable marine settings spanning open-ocean to continental shelf environments that permit
367 assessment of species diversity, population abundances and faunal turnovers. Census data are
368 summarized in Table 1 as cumulative species diversity per biozone.
369
370 **5.1 Diversity Maximum: Early Maastrichtian**
371
372 In the Indian Ocean, the early Maastrichtian zones CF8-CF5 reveal 14 species
373 originations at Site 217 (Fig. 6) and 16 species originations at the Cauvery Basin well Kali-H

374 (Fig. 7). Note that in these sections only part of zone CF8 is present but the number of species
375 originations not yet reached at these sites can still be estimated based on Tunisia and Site 525A.
376 At El Kef, 21 species originations occurred in the early Maastrichtian, which is comparable to
377 Elles with 18 species (Fig. 8). At Site 525A, 23 species originations are identified during this
378 interval (Fig. 9). Most of these species are also present in the Indian Ocean Site 217 and Kali-H
379 but the first appearances of some are not recorded because of incomplete core recovery. If we
380 add those first appearances, then species originations at Site 217 and Kali-H increase to 22 and
381 25 species, respectively (Table 1). Elles and Site 525A also show 7 and 6 species originations in
382 zones CF9-CF8b, indicating gradual diversification already beginning in the latest Campanian.
383 Most of the species originations occurred among subsurface and thermocline dwellers.
384 The latter probably originated as subsurface dwellers that later migrated to thermocline depths
385 during warm intervals and increased water mass stratification (Abramovich et al., 2003).
386 Originations are likely due to a major increase in nutrient availability driving primary
387 productivity (Fig. 5) and faunal diversification (Hallock, 1987). Ninety East Ridge volcanism
388 was probably a major contributor of nutrients in the Indian Ocean as suggested by the inferred
389 total number of species originations (22 at Site 217, 25 at Kali-H; Table 1) although recovery is
390 incomplete for the base CF8-CF9 interval (Figs. 6, 7). Maximum diversity is reached during the
391 CF6/CF5 transition in Kali-H and Elles, and in the lower part of zone CF4 at Sites 217 and 525A.

At El Kef, the diversity maximum is at the base of CF3, but the late Maastrichtian record is suspect because of major faults in the area that complicate stratigraphy (Li and Keller, 1998c).

5.2 Minor Extinction Event: Early to Late Maastrichtian

A minor extinction event coincides with the end of climate warming in the early late Maastrichtian and is commonly known as "mid-Maastrichtian event" (e.g., MacLeod, 1994; Barrera and Savin, 1999; Li and Keller, 1998a, 1999; Nordt et al., 2003; Frank et al., 2005; Friedrich et al., 2009; Keller et al., 2016a; Thibault, 2016). This mid-Maastrichtian event is also observed in all sections analyzed for this study.

At Site 217, this minor extinction event is observed at the CF4/CF3 transition and marked by the disappearances of *Contusotruncana fornicata*, *C. plummerae* and *Globotruncana bulloides*, with *Archeoglobigerina cretacea* and *Gublerina acuta* disappearing in zone CF3 above the CF4/CF3 hiatus (Fig. 6). In the Cauvery Basin Kali-H well, this event also includes the disappearances of *C. fornicata*, *C. plummerae*, as well as *A. cretacea*, *G. acuta* and *Globotruncana esnehensis*. Because the latter two species are known to range higher in the stratigraphic record (e.g., Li and Keller, 1998a; Abramovich and Keller, 2002; Abramovich et al., 2002; Darvishzad et al., 2007; Huber et al., 2008; Punekar et al., 2014b), their early

410 disappearance in the Indian Ocean suggests regional differences (e.g., diachronous occurrences)
411 in species ranges.

412 At El Kef and Elles, the disappearances of *C. fornicata* and *C. plummerae* occur in zone
413 CF5, rather than CF4 (Fig. 8). At El Kef, this may be due to the incomplete Maastrichtian record
414 cut by major faults, but at Elles the late Maastrichtian is undisturbed, suggesting that the zone
415 CF4 index species *R. fructicosa* may be diachronous in the shallower middle shelf environment,
416 or that high-stress conditions were more severe in shallower environments (e.g., Leckie, 1987).
417 At Site 525A, *C. fornicata*, *G. bulloides*, *C. plummerae*, *A. cretacea* and *Globotruncana*
418 *ventricosa* gradually disappear in zone CF4 (Fig. 9). This minor extinction event has also been
419 recorded in Madagascar, Israel, Egypt and Poland (Abramovich et al., 2002, 2010; Dubicka and
420 Peryt, 2012; Punekar et al, 2014b; Keller et al., 2016a). From shallow to deep environments, this
421 faunal turnover seems to have been the result of global environmental perturbations that coincide
422 with the transition from warm to cool climate (Fig. 5) associated with reduced water mass
423 stratification, increased competition and biotic stress leading to the extinction of specialized
424 subsurface and thermocline dwelling species.

425

426 **5.3 Late Maastrichtian Diversity Decline preceding the Mass Extinction**

427

A major faunal turnover in species populations, but minor change in species diversity, is generally observed in zone CF3 (Figs. 6-8) correlative with maximum cooling, suggesting increased stress conditions as evident by the decreased relative abundances of specialist species and increased abundance of generalist species more tolerant of environmental changes (further discussed in Section 6.1). In zones CF2-CF1, diversity gradually decreased along with further reduction in specialist species populations prior to the very rapid mass extinction at the K/T boundary (Figs. 8, 9). Environmental changes in zones CF2-CF1 have been widely studied and recently linked to the massive Deccan eruptions and volcanic degassing that led to climate warming, eutrophication and ocean acidification contributing to this major biotic crisis (e.g., Punekar et al., 2014a, 2016; Font et al., 2014, 2016; Thibault, 2016).

6 ENVIRONMENTAL EFFECTS

6.1 Ecological Associations and Depth Ranking

Planktic foraminiferal assemblages consist of three main ecological groups: specialists, generalists and disaster opportunists. Specialists species, known as K-strategists, are diverse species with large, complex tests, that tolerate a narrow range of environmental conditions, have

446 long life spans and produce a small number of offspring (Begon et al., 1996, 1998). A common
447 group of K-strategists includes species of the genera *Abathomphalus*, *Archeoglobigerina*,
448 *Contusotruncana*, *Globotruncana*, *Globotruncanita*, *Gublerina*, *Planoglobulina*,
449 *Pseudoguembelina*, *Pseudotextularia*, *Racemiguembelina* and *Rugoglobigerina* (Premoli Silva
450 and Sliter, 1999; Keller and Abramovich, 2009). These species are most abundant in stable
451 environments with oligotrophic conditions, which foster optimum assemblages with high species
452 diversity, a variety of test sizes, morphologies and ornamentation (e.g., Premoli Silva and Sliter,
453 1999; Pardo and Keller, 2008; Keller and Abramovich, 2009).

454 Generalist and disaster opportunist species are known as ecological R-strategists: low-
455 diversity species assemblages with relatively small, simple tests, able to occupy a wide range of
456 ecological niches, have shorter life spans and produce larger numbers of offspring, thus
457 maximizing their chance for survival (Begon et al., 1996, 1998; Premoli Silva and Sliter, 1999;
458 Keller and Abramovich, 2009). Generalists are represented by species of the genera
459 *Globigerinelloides*, *Globotruncanella*, *Hedbergella* and *Heterohelix*. They tend to dominate
460 high-stress environments affected by temperature, salinity, nutrients and oxygen variations in
461 which large specialized species struggle to survive. *Heterohelix* species are common under
462 mesotrophic conditions in low oxygen environments, usually thriving during times of an
463 expanded oxygen minimum zone (OMZ) (Pardo and Keller, 2008), while *Globigerinelloides*

species are most abundant in extreme eutrophic conditions (Ashckenazi-Polivoda et al., 2011). Disaster opportunists, such as *Guembelitria* species, thrived under the most severe biotic stress conditions generally associated with mesotrophic to eutrophic conditions in shallow continental shelves, upwelling areas and volcanically influenced regions (e.g., Kroon and Nederbragt, 1990; Koutsoukos, 1994; Coccioni and Luciani, 2006; Pardo and Keller, 2008; Keller and Abramovich, 2009; Ashkenazi-Polivoda et al., 2014; Punekar et al., 2014a).

Planktic foraminifera also occupy a wide variety of ecological niches at various depths in the water column. Previous studies determined species depth ranking in the water column based on their oxygen and carbon isotopic signals and grouped them into surface, subsurface, thermocline and deep dwellers (Abramovich et al., 2003, 2011; Ashkenazi-Polivoda et al., 2014). Diversity and abundance changes for each depth group can be used to interpret changes in climate and water mass stratification as well as paleoecology.

At Site 217, generalist species dominate the 63-150 μm size fraction, particularly *Heterohelix* and *Globigerinelloides* species, which are most abundant from zone CF8 to CF5 and from zone CF4 to CF3, respectively (Fig. 10), suggesting mesotrophic to eutrophic surface water conditions. A significant increase, from 4 % to 13 %, in *Globotruncanella* species is observed in zone CF3 in the predominantly smaller 63-150 μm size fraction, indicating dwarfing due to increased biotic stress. Specialist species are the second-most abundant group in the assemblage

with dwarfed pseudoguembelinids dominating. Disaster opportunist *Guembelitria cretacea* is present throughout the section but rare (<1 %) except for the upper part of zone CF4 through CF3 and CF2 where relative abundances average 5 %; maximum peaks of 43 % are observed in zone CF2 in the dwarfed 38-63 μm size fraction (Fig. 10). This increased abundance indicates increasing environmental stress mainly in zones CF3-CF2 compared with the lower part of the section. Overall, dwarfed specialists (pseudoguembelinids), a marked faunal turnover at the CF4/CF3 transition, and presence of dwarfed *Guembelitria* with peak abundance in zone CF2 reveal increased biotic and environmental stress conditions from the early to the late Maastrichtian.

The >150 μm size fraction is dominated by specialist species with different degrees of environmental tolerance. Pseudoguembelinids, which are the only large surface dwellers with significant abundance, appear to be the most tolerant as evident by their maximum abundance (6.5 % to 32 %) during the increasingly high-stress environment of zones CF3-CF2 (Fig. 11). In contrast, the subsurface and thermocline dwelling globotruncanids appear less tolerant of environmental fluctuations as indicated by their permanent decrease beginning in zone CF3. A similar lack of tolerance in CF3-CF2 environments is observed in the subsurface dwelling rugoglobigerinids. Reduced abundance of subsurface dwellers appears to be the result of reduced water mass stratification that led to decreased ecological niches and increased competition.

Small heterohelicids generally dominate among generalists, *H. globulosa, H. planata, and H. (Paraspiroplecta) navarroensis*, but *Gublerina rajagopalani*, a deep dweller, is the most abundant species in the larger >150 μm size fraction at Site 217 (Fig. 11). The high abundance of this large, robust and thick-walled species may be attributed primarily to selective preservation during carbonate dissolution. Noteworthy is the peak in the surface dweller *Guembelitria* in the 38-63 μm size fraction in zone CF2 (Fig. 10) coincident with dominance of large surface dwellers in the >150 μm size fraction (Fig. 11b), which suggests further reduction in habitats for deeper dwellers. Stable isotope ranking shows that *Guembelitria* thrived at the very sea-surface (Pardo and Keller, 2008; Abramovich et al., 2011; Ashkenazi-Polivoda et al., 2014) where CO_2 uptake from the air mitigates ocean acidification that affects other surface and subsurface dwellers. All of these species population changes indicate increased high-stress environments beginning in CF4, increasing through CF3 and further increasing in CF2, as a result of reduced water mass stratification, reduced ecological niches and increased carbonate dissolution for planktic foraminifera.

6.2 Dwarfing

517 Species dwarfing refers to size reductions as a result of high-stress environments
518 commonly associated with rapid climate change, perturbations in the water column and/or
519 mesotrophic conditions (Abramovich and Keller, 2003; Keller and Abramovich, 2009). It is a
520 survival response that enhances reproduction rates through early sexual maturation (i.e.,
521 organisms reach reproductive adulthood much below normal size; MacLeod et al., 2000; Keller
522 and Abramovich, 2009).

523 At Site 217, there is a gradual trend throughout the section towards increased dwarfing
524 suggesting a progressive increase in high-stress environmental conditions (Fig. 12). In zone CF8,
525 the assemblage in the >150 μm size fraction is dominated by specimens >250 μm in size
526 averaging 72 %. From zones CF7 to CF3, specimens in the 150-250 μm group are more
527 abundant with an average of 52 %. In zone CF2, dwarfed specimens dominate averaging 60 % in
528 the 150-250 μm group but several horizons have <50 specimens (e.g., 424.08 m, 424.59 m,
529 425.19 m, 426.70 m, 432.96 m). This indicates more severe environmental conditions associated
530 with increased competition due to reduced water mass stratification and possibly carbonate
531 dissolution. Similar results have been reported from wells in the Cauvery Basin, India, where
532 planktic foraminifer diversity drops sharply and species tend to be dwarfed in the upper part of
533 zone CF3 pointing to high biotic stress (Keller et al., 2016b).

534

6.3 Dissolution (Fragmentation Index)

Preservation of planktic foraminiferal tests is mainly controlled by 1) seawater saturation with respect to $CaCO_3$ in the water column, and 2) the amount of organic matter buried in $CaCO_3$ rich sediments (e.g., Emerson and Bender, 1981). Dissolution is assessed based on 1) fragmentation index, 2) preferential preservation of robust planktic foraminiferal morphologies (species-selective dissolution), and 3) planktic/benthic (P/B) ratio of foraminifera (e.g., Parker and Berger, 1971; Thunell, 1976). The fragmentation index is calculated using the percentage of planktic foraminiferal fragments relative to the total number of whole tests and consists of three categories, "good", "fair" and "poor" based on the quality of preservation: good = nearly perfect tests, fair = imperfect tests, and poor = fragments (Punekar et al., 2016).

At Site 217, the "fair" group is the most abundant resulting in ~58 % from zone CF8 to the lower part of zone CF4 (Fig. 12). The "poor" group increases in the upper part of zone CF4 and dominates (91 %) in CF3. In contrast, zone CF2 is dominated by the "fair" group (~48 %), similar to lower CF4. Just below the hiatus in CF2 at the top of the section, the "poor" group dominates (70 %). The "good" group is a relatively minor component and maintains an average of only 13 %.

These results indicate that dissolution effects are most severe in zone CF3, as also evident by the dominance of robust, thick-walled and dissolution-resistant planktic species (e.g., *G. rajagopalani*, *P. palpebra* and *A. mayaroensis*, Fig. 3). Climate cooling in zone CF3 and the accompanying intensified bottom water circulation likely exacerbated effects of dissolution as suggested by the fragmentation of most foraminifera in this interval. Relative abundance of benthic compared to planktic foraminifera increase from 9 % in zones CF8-CF5 to 46 % in zone CF4 and dominate in zones CF3-CF2 with an average of 61 % (Fig. 12). These results reveal that at Site 217 increased dissolution actually started in zone CF4 and was persistent through CF2, as benthic foraminifera are less vulnerable to dissolution than planktic foraminifera. Planktic foraminifera dominate again (90 %) just below the KTB hiatus in zone CF2, coincident with increased abundance of surface dwellers, including peak abundance of the disaster opportunist *Guembelitria cretacea* (Figs. 10, 11). This suggests severe high-stress environmental conditions detrimental to all but sea-surface dwellers. Ocean acidification and reduced water mass stratification are likely contributors to the biotic stress that affected planktic foraminiferal assemblages during zones CF4-CF2.

7. MAASTRICHTIAN CLIMATE AND FAUNAL EVENTS

570 The Cretaceous greenhouse warming ended in the late Campanian with global cooling
571 that reached minimum temperatures in the earliest Maastrichtian (base C31r) accompanied by
572 low primary productivity and low diversity in planktic foraminifera (Fig. 13) (e.g., Li and Keller,
573 1998a; Huber et al., 2002; Friedrich et al., 2009). From the latest Campanian through the
574 Maastrichtian, four major climate and faunal events are identified in the South Atlantic, Tethys
575 and Indian Oceans: (1) minimum diversity in the late Campanian to earliest Maastrichtian
576 followed by unprecedented diversification for the Cretaceous reaching maximum in the early
577 Maastrichtian (Event-1, C31r), (2) a period of warming and stable high diversity (Event-2, upper
578 C31r to lower C30n), (3) return to global cooling and high-stress environments (Event-3, C30n),
579 and (4) rapid global warming and severe stress conditions in the late Maastrichtian preceding the
580 K/T mass extinction (Event-4, C29r). Here we summarize these climate and faunal events based
581 on stable isotopes and diversity records of South Atlantic Site 525A (Li and Keller, 1998a)
582 compared with diversity curves from four localities in the Tethys and Indian oceans (Fig. 13).
583
584 **7.1 Event-1: Early Maastrichtian Cooling and Diversification**
585
586 The prelude to Event-1 is the late Campanian climate cooling (C32n, zones CF9-CF8)
587 when bottom water temperatures dropped from 16 °C to 10 °C, surface water temperatures from

22 °C to 17 °C, and primary productivity and planktic foraminiferal diversity were relatively low (Fig. 13) (Li and Keller, 1998a). Event-1 spans most of the early Maastrichtian (zones CF8b-CF6, C31r) with steady cold bottom water temperatures and gradual cooling of surface waters. $\delta^{13}C$ values rapidly increased by +1 ‰ and +1.4 ‰ in bottom and surface waters, respectively, indicating a major increase in primary productivity. Increasing primary productivity in the early Maastrichtian is also observed in northern middle to high latitudes as indicated by calcareous nannofossils and benthic foraminiferal assemblages (Friedrich et al., 2005). At Site 217, primary productivity was already high due to nutrient influx from Ninety East Ridge (Fig. 5). Planktic foraminifera responded with rapid evolutionary diversification among subsurface and thermocline dwellers (Fig. 13). Species originations vary from 45 % to 57 % (e.g., low of 35-42 to high of 55-61 species) among the five localities analyzed.

What could have caused the diversity decrease during the late Campanian cooling and the rapid diversification during the subsequent maximum cooling of the early Maastrichtian? The late Campanian cooling that ended the late Cretaceous greenhouse world is commonly attributed to a combination of declining atmospheric CO_2 related to decreasing oceanic crust production and the opening of ocean gateways that profoundly affected deep, intermediate and shallow waters circulation patterns (review in Linnert et al., 2014). Specialist planktic foraminifera were ill-suited to adapt to these environmental changes and many disappeared. By the earliest

606 Maastrichtian maximum cooling, decreased diversity, reduced competition and high nutrient
607 availability created favorable conditions for species originations (Li and Keller, 1998a, c). High
608 nutrient inputs were likely due to several factors including (1) increased temperature gradient
609 between equator and poles favoring development of zonal winds and thus coastal upwelling of
610 nutrient-rich waters (e.g., Vincent and Berger, 1985; Zachos et al., 1993), (2) increased erosion
611 and nutrient influx from the continents during the sea-level lowstand ~70.6 Ma (Haq, 2014), and
612 (3) nutrient inputs from Ninety East Ridge volcanic activity (e.g., Vermeij, 1995) active since
613 ~82 Ma (Coffin et al, 2002; Pringle et al., 2008).
614
615 **7.2 Event-2: Mid-Maastrichtian Warming, Maximum Diversity, Extinctions**
616
617 Event-2, also known as mid-Maastrichtian event, begins near the end of the early
618 Maastrichtian and persists through upper zones CF6 to middle CF4 (C31n) (Fig. 13). Bottom and
619 surface waters warmed by 2-3 °C and terrestrial temperatures peaked at 22 °C (e.g., Li and
620 Keller, 1998a; Zepeda, 1998; Nordt et al., 2003; Thibault and Gardin, 2007). High primary
621 productivity and maximum diversity in planktic foraminifera persisted through this interval (Li
622 and Keller, 1998a). The cause for this warming, attributed to abrupt reorganization of
623 intermediate oceanic circulation, has long been an enigma (Frank and Arthur, 1999; Li and

624 Keller, 1999), but recent studies suggest the cause could have been Ninety East Ridge volcanism
625 (Keller et al., 2016a). An intense phase of volcanic activity is recorded at DSDP Site 216
626 beginning ~69.5 Ma and spanning zones CF5-CF3 coincident with persistent maximum diversity,
627 high primary productivity, climate warming and increased water mass stratification favoring
628 planktic foraminiferal evolution (Keller, 2005; Tantawy et al., 2009).

629 Deccan volcanism began near the end of Event-2 at the base of C30n (~67.1 Ma, Schöbel
630 et al., 2014) further contributing to intense greenhouse warming and acid rains enhancing the
631 delivery of nutrients to the oceans, thus resulting in mesotrophic conditions in surface waters
632 favoring primary productivity. Faunal responses to these high-stress conditions include peak
633 abundance of the disaster opportunist *Guembelitria cretacea*, and onset of the terminal decrease
634 in large specialized globotruncanid species.

635 Enhanced weathering and probably waning volcanism eventually lowered volcanic CO_2
636 levels in the atmosphere resulting in climate cooling (e.g., Dessert et al., 2001), as observed in
637 the upper part of zone CF4 (Fig. 13). Cooling would have further affected planktic foraminiferal
638 assemblages by leading to reduced water mass stratification as temperature gradients between
639 surface and deep waters decreased (e.g., Doney et al., 2012), thus resulting in reduced ecological
640 niches and disappearance of some species (e.g., minor extinction event), marking the end of
641 diversification.

642

643 **7.3 Event-3: Late Maastrichtian Cooling and Diversity Decline**

644

645 Renewed global cooling during the late Maastrichtian upper zone CF4 to CF3 (C30n)
646 marks Event-3 accompanied by sustained high primary productivity but increasingly high-stress
647 marine environments for planktic foraminifera as a result of reduced ecological niches
648 exacerbated by ocean acidification evident in increased carbonate dissolution effects (Figs. 12,
649 13). Faunal responses include species dwarfing, decreased populations of specialized species,
650 temporary exclusions, dominance by generalist and/or disaster opportunist species and general
651 diversity decrease, as observed in the Indian Ocean, Tethys and South Atlantic Oceans.

652 What caused the diversity decline during cooling in the late Maastrichtian instead of a
653 diversity increase as observed during the early Maastrichtian cooling? Volcanism was active on
654 Ninety East Ridge and in India (Deccan phase-1) but on relatively reduced levels during zone
655 CF3 (C30n; Keller, 2005; Chenet et al., 2009) and insufficient to sustain global warming but
656 sufficient to cause persistent ocean acidification, which stressed already reduced habitats. Large
657 amounts of volcanogenic CO_2 adsorpt by the oceans changes seawater chemistry by lowering
658 carbonate ion (CO_3^{2-}) concentration, surface ocean pH and saturation states of calcium carbonate
659 minerals (Kump et al., 2009). The result is a carbonate crisis (i.e., decrease in $CaCO_3$ production)

660 that significantly affects marine ecosystems, particularly marine calcifiers such as foraminifera
661 (reviews in Doney et al., 2009; Hönisch et al., 2012). At Site 217, dissolution due to surface
662 ocean acidification led to thinner planktic foraminiferal tests, thus more vulnerable to breakage
663 (e.g., Moy et al., 2009), resulting in the high fragmentation index observed in zone CF3 (Fig. 12).
664 Dissolution effects in other localities have not been routinely recorded and still have to be
665 evaluated, although similar effects have been observed in zones CF4-CF3 in the Cauvery Basin
666 (Keller et al., 2016b) and Site 525A (Punekar et al., unpublished data). Enhanced weathering and
667 a major sea-level fall (~66.8 Ma) accompanied by widespread erosion also contributed to global
668 cooling as well as increased nutrient input into the oceans leading to mesotrophic conditions,
669 detrimental to planktic foraminifera.
670
671 **7.4 Event-4: Latest Maastrichtian Rapid Climate Warming and Mass Extinction**
672
673 Event-4 marks the last 250 kyr of the Maastrichtian (zones CF2-CF1, C29r), beginning
674 with the largest Deccan eruptions (Phase-2) that caused rapid climate warming of 4 °C in bottom
675 and surface waters and 8 °C on land, acid rain and ocean acidification leading to a major
676 carbonate crisis thus contributing to the mass extinction (reviews in Punekar et al., 2014a; Keller
677 et al., 2016a). This event is not present at Site 217 and rarely present in other Indian Ocean

678 localities due to a major hiatus. The K/T boundary is also missing in the South Atlantic (DSDP
679 Site 525A) and is fragmented in the Tethys (Egypt and Israel) although the best records are
680 preserved in Tunisia (Fig. 2). This interval has been discussed in several recent publications in
681 which Deccan volcanism is directly associated to the K/T mass extinction in India (Keller et al.,
682 2011; Gertsch et al., 2011), U-Pb dating of lava flows narrow the main phase of eruptions to just
683 250 kyr below the KTB (Schoene et al., 2015), and global faunal and geochemical studies point
684 to Deccan volcanism as a major trigger of the K/T mass extinction (e.g., Font et al., 2014, 2016;
685 Punekar et al., 2014a, 2016), whereas others proposed a link between accelerated Deccan
686 volcanism and the Chicxulub impact (Richards et al., 2015; Renne et al., 2015).
687
688 **8 CONCLUSIONS**
689
690 From the latest Campanian through the Maastrichtian, four major climate and faunal
691 events are identified that ultimately ended with the K/T mass extinction.
692 • Event-1: Maximum cooling in the early Maastrichtian (zones CF8b-lower CF6; C31r) is
693 associated with rapid planktic foraminiferal species originations reaching maximum
694 Cretaceous diversity as a result of increased nutrient input due to enhanced upwelling,
695 costal erosion and/or volcanic activity.

- Event-2: Warming during the early/late Maastrichtian transition (mid-Maastrichtian event; CF5 to lower CF4; upper C31r-C31n) is attributed to Ninety East Ridge volcanic activity that records an intense phase of eruptions at Site 216 in zones CF5-CF3. Warming led to increased water mass stratification that sustained maximum diversity.
- A minor extinction event ends Event 2 and marks the onset of increasingly more stressful marine conditions for planktic foraminifera particularly specialized species living in subsurface and thermocline depths.
- Event-3: Return to maximum cooling in zone CF3 (C30n) increased stress conditions for marine calcifiers leading to reduced specialized species populations, dwarfing, and dominance of smaller ecological generalists able to tolerate ongoing environmental changes. The global cooling and faunal turnover likely resulted from increased CO2 uptake by the oceans as a result of Ninety East Ridge and Deccan Trap volcanism, increased weathering after the greenhouse warming in the early-late Maastrichtian transition, ocean acidification and mesotrophic conditions.
- Event-4: Massive Deccan volcanic eruptions (phase-2) in zones CF2-CF1 spanning the last 250 kyr of the Maastrichtian (C29r) coincident with increasingly high-stress environments, decreasing abundance of large specialized species and dominance of the

disaster opportunist *Guembelitria cretacea*. In the Indian Ocean, South Atlantic and eastern Tethys a major KTB hiatus is present.

- Positive and negative effects observed in planktic species diversification and population abundance variations through the Maastrichtian can be linked to volcanism. Positive effects correlate with increased nutrient input, increased water mass stratification and increased ecological niches during climate warming. Negative effects can be linked to increased tempo and rate of volcanism resulting in ocean acidification, carbonate crisis and extinction.

ACKNOWLEDGMENTS

This study is based upon work supported by Princeton University, Geosciences Department Tuttle and Scott funds; the US National Science Foundation through the Continental Dynamics Program (Leonard Johnson), Sedimentary Geology and Paleontology Program (Richard Lane) and Office of International Science & Engineering's India Program under NSF Grants EAR-0207407, EAR-0447171 and EAR-1026271. We thank India's Oil and Natural Gas Corporation for permission to publish analysis of the Cauvery Basin core.

730 Special thanks to the reviewers, Nicolas Thibault and Sarit Ashckenazi-Polivoda, and editors,

731 David Bond and Thomas Algeo, for their insightful comments and suggestions.

REFERENCES

Abramovich, S., and Keller, G., 2002. High stress late Maastrichtian paleoenvironment: inference from planktonic foraminifera in Tunisia. Palaeogeography, Palaeoclimatology, Palaeoecology, 178, 145-164, doi:10.1016/S0031-0182(01)00394-7.

Abramovich, S., and Keller, G., 2003. Planktonic foraminiferal response to the latest Maastrichtian abrupt warm event: A case study from South Atlantic DSDP Site 525A. Marine Micropaleontology, 48(3-4), 225-249, doi:10.1016/S0377-8398(03)00021-5.

Abramovich, S., Almongi-Labin, A., and Benjamini, C., 1998. Decline of the Maastrichtian pelagic ecosystem based on planktic foraminifera assemblage changes: implication for the terminal Cretaceous faunal crisis. Geology, 26, 63-66, doi:10.1130/0091-7613(1998)026b0063:DOTMPEN2.3.CO;2.

Abramovich, S., Keller, G., Adatte, T., Stinnesbeck, W., Hottinger, L., Stüben, D., Berner, Z., Ramanivosoa, B., and Randriamanantenasoa, A., 2002. Age and paleoenvironment of the Maastrichtian–Paleocene of the Mahajanga Basin, Madagascar: a multidisciplinary approach. Marine Micropaleontology, 47, 17-70, doi:10.1016/S0377-8398(02)00094-4.

Abramovich, S., Keller, G., Stüben, D., and Berner, Z., 2003. Characterization of late Campanian and Maastrichtian planktonic foraminiferal depth habitats and vital activities based on

stable isotopes. Palaeogeography, Palaeoclimatology, Palaeoecology, 202, 1-29, doi:10.1016/S0031-0182(03)00572-8.

Abramovich, S., Yovel-Corem, S., Almogi-Labin, A., and Benjamini, C., 2010. Global climate change and planktic foraminiferal response in the Maastrichtian. Paleoceanography, 25, PA2201, doi:10.1029/2009PA001843.

Abramovich, S., Keller, G., Berner, Z., Cymbalista, M., and Rak, C., 2011. Maastrichtian planktic foraminiferal biostratigraphy and paleoenvironment of Brazos River, Falls County, Texas. In: Keller, G., Adatte, T. (Eds.), The End-Cretaceous Mass Extinction and the Chicxulub Impact in Texas. Society for Sedimentary Geology Special Publication 100, pp. 123-156, ISBN: 978-1-56576-308-1.

Alvarez, L.W., Alvarez, W., Asaro, F., and Michel, H.V., 1980. Extraterrestrial cause for the Cretaceous-Tertiary extinction. Science, 208, 1095-1108, doi: 10.1126/science.208.4448.1095.

Alvarez, L.W., 1983. Experimental evidence that an asteroid impact led to the extinction of many species 65 million years ago. Proceedings of the National Academy of Sciences, 80(2), 627-642.

Arenillas, I., Arz, J.A., Grajales-Nishimura, J.M., Murillo-Muneton, G., Alvarez, W., Camargo-Zanguera, A., Molina, E., and Rosales-Dominguez, C., 2006. Chicxulub impact event is

768 Cretaceous/Paleogene boundary in age: New micropaleontological evidence. Earth and
769 Planetary Science Letters, 249, 241-257, doi:10.1016/j.epsl.2006.07.020.
770 Ashckenazi-Polivoda, S., Abramovich, S., Almogi-Labin, A., Schneider-Mor, A., Feinstein, S.,
771 Püttmann, W., and Berner, Z., 2011. Paleoenvironments of the latest Cretaceous oil shale
772 sequence, Southern Tethys, Israel, as an integral part of the prevailing upwelling system.
773 Palaeogeography, Palaeoclimatology, Palaeoecology, 305(1), 93-108,
774 doi:10.1016/j.palaeo.2011.02.018.
775 Ashckenazi-Polivoda, S., Rak, C., Almogi-Labin, A., Zsolt, B., Ovadia, O., and Abramovich, S.,
776 2014. Paleoecology of the K-Pg mass extinction survivor Guembelitria (Cushman):
777 isotopic evidence from pristine foraminifera from Brazos River, Texas (Maastrichtian).
778 Paleobiology, 40(1), 24-33, doi:10.1666/13317.
779 Barrera, E., 1994. Global environmental changes preceding the Cretaceous-Tertiary boundary:
780 Early-late Maastrichtian transition. Geology, 22(10), 877-880, doi: 10.1130/0091-
781 7613(1994)022<0877:GECPTC>2.3.CO;2.
782 Barrera, E., and Huber, B.T., 1990. Evolution of Antarctic waters during the Maastrichtian:
783 Foraminifer oxygen and carbon isotope ratios, Leg 113. In: Barker, P.F., Kennett, J.P.
784 (Eds.), Proceedings of the Ocean Drilling Program, Scientific Results, 113. College Station,
785 Texas, Ocean Drilling Program, pp. 813-827.

786 Barrera, E., and Savin, S.M., 1999. Evolution of late Campanian-Maastrichtian marine climates
787 and oceans. In: Barrera, E., Johnson, C.C. (Eds.), Evolution of the Cretaceous Ocean-
788 Climate System. Geological Society of America Special Papers, 332, pp. 245-282.
789 Barrera, E., Huber, B.T., Savin, S.M., and Webb, P.N., 1987. Antarctic marine temperatures:
790 Late Campanian through early Paleocene. Paleoceanography, 2(1), 21-47,
791 doi:10.1029/PA002i001p00021.
792 Begon, M., Mortimer, M., and Thompson, D.J., 1996. Population Ecology: A Unified Study of
793 Plants and Animals. Cambridge, UK, Blackwell, 247 p.
794 Begon, M., Harper, J.L., and Townsend, C.R., 1998. Ecology: Individuals, Populations and
795 Communities. Boston, Blackwell Science, 1068 p.
796 Bond, D.P.G., and Wignall, P.B., 2014. Large igneous provinces and mass extinctions: An
797 update. In: Keller, G., Kerr, A.C. (Eds.), Volcanism, Impacts, and Mass Extinctions:
798 Causes and Effects. Geological Society of America Special Paper, 505, 29-55,
799 doi:10.1130/2014.2505(02).
800 Bralower, T.J., Paull, C.K., and Leckie, R.M., 1998. The Cretaceous-Tertiary boundary cocktail:
801 Chicxulub impact triggers margin collapse and extensive sediment gravity flows. Geology,
802 26(4), 331-334, doi:10.1130/0091-7613(1998)026<0331:TCTBCC>2.3.CO;2.

803 Burnett, J., 1998. Upper Cretaceous. In: Bown, P.R. (Ed.), Calcareous Nannofossil
804 Biostratigraphy. Chapman & Hall, Cambridge, pp. 132-199.
805 Chenet, A.-L., Quidelleur, X., Fluteau, F., Courtillot, V., and Bajpai, S., 2007. 40K/40Ar dating
806 of the main Deccan large igneous province: Further evidence of Cretaceous-Tertiary
807 boundary age and short duration. Earth and Planetary Science Letters, 263, 1-15,
808 doi:10.1016/j.epsl.2007.07.011.
809 Chenet, A.-L., Fluteau, F., Courtillot, V., Gérard, M., and Subbarao, K.V., 2008. Determination
810 of rapid Deccan eruptions across the Cretaceous-Tertiary boundary using paleomagnetic
811 secular variation: results from a 1200-m-thick section in the Mahabaleshwar escarpment.
812 Journal of Geophysical Research: Solid Earth, 113(B4), doi:10.1029/2006JB004635.
813 Chenet, A.-L., Courtillot, V., Fluteau, F., Gerard, M., Quidelleur, X., Khadri, S.F.R., Subbarao,
814 K.V., and Thordarson, T., 2009. Determination of rapid Deccan eruptions across the
815 Cretaceous-Tertiary boundary using paleomagnetic secular variation: 2. Constraints from
816 analysis of eight new sections and synthesis for a 3500-m-thick composite section. Journal
817 of Geophysical Research: Solid Earth, 114(B6), doi:10.1029/2008JB005644.
818 Coccioni, R., and Luciani, V., 2006. Guembelitria irregularis bloom at the K-T boundary:
819 morphological abnormalities induced in planktonic foraminifera by impactrelated extreme

environmental stress? In: Cockell, C., Gilmour, I., Koeberl, C. (Eds.), Biological Processes Associated with Impact Events. Springer-Verlag, Berlin, pp. 179-196.

Coffin, M.F., 1992. Emplacement and subsidence of Indian Ocean plateaus and submarine ridges. In: Duncan, R.A., et al. (Eds.), Synthesis of results from scientific drilling in the Indian Ocean, 115-125, doi:10.1029/GM070p0115.

Coffin, M.F., Pringle, M.S., Duncan, R.A., Gladczenko, T.P., Storey, M., Müller, R.D., and Gahagan, L.A., 2002. Kerguelen hotspot magma output since 130 Ma. Journal of Petrology, 43(7), 1121-1137, doi:10.1093/petrology/43.7.1121.

Courtillot, V., and Fluteau, F., 2014. A review of the embedded time scales of flood basalt volcanism with special emphasis on dramatically short magmatic pulses. In: Keller, G., Kerr, A.C. (Eds.), Volcanism, Impacts, and Mass Extinctions: Causes and Effects. Geological Society of America Special Paper, 505, SPE505-15, doi:10.1130/2014.2505(15).

Courtillot, V., and Renne, P.R., 2003. On the ages of flood basalt events. Comptes Rendus Geoscience, 335(1), 113-140, doi:10.1016/S1631-0713(03)00006-3.

Culver, S.J., 2003. Benthic foraminifera across the Cretaceous–Tertiary (K–T) boundary: a review. Marine Micropaleontology, 47(3), 177-226, doi:10.1016/S0377-8398(02)00117-2.

836 Darvishzad, B., Ghasemi-Nejad, E., Ghourchaei, S., and Keller, G., 2007. Planktonic
837 foraminiferal biostratigraphy and faunal turnover across the Cretaceous-Tertiary boundary
838 in southwestern Iran. Journal of Sciences, Islamic Republic of Iran, 18(2), 139-149.
839 Dessert, C., Dupré, B., François, L.M., Schott, J., Gaillardet, J., Chakrapani, G., and Bajpai, S.,
840 2001. Erosion of Deccan Traps determined by river geochemistry: impact on the global
841 climate and the 87 Sr/86 Sr ratio of seawater. Earth and Planetary Science Letters, 188(3),
842 459-474, doi:10.1016/S0012-821X(01)00317-X.
843 D'Hondt, S., and Arthur, M.A., 2002. Deep water in the late Maastrichtian ocean.
844 Paleoceanography, 17(1), doi:10.1029/1999PA000486.
845 Doney, S.C., Fabry, V.J., Feely, R.A., and Kleypas, J.A., 2009. Ocean acidification: The other
846 CO2 problem. Annual Review of Marine Science, 1, 169-192,
847 doi:10.1146/annurev.marine.010908.163834.
848 Doney, S.C., Ruckelshaus, M., Duffy, J.E., Barry, J.P., Chan, F., English, C.A., Galindo, H.M.,
849 Grebmeier, J.M., Hollowed, A.B., Knowlton, N., Polovina, J., Rabalais, N.N., Sydeman,
850 W.J., Talley, L.D., 2012. Climate change impacts on marine ecosystems. Marine Science, 4,
851 11-37, doi:10.1146/annurev-marine-041911-111611.
852 Douglas, R.G., and Savin, S.M., 1975. Oxygen and carbon isotope analyses of Tertiary and
853 Cretaceous microfossils from Shatsky Rise and other sites in the North Pacific Ocean.

854 Initial reports of the deep sea drilling project, 32, 509-520,
855 doi:10.2973/dsdp.proc.32.115.1975.
856 Dubicka, Z., and Peryt, D., 2012. The Lower/Upper Maastrichtian boundary interval in the
857 Lublin Syncline (SE Poland, Boreal realm): new insight into foraminiferal stratigraphy.
858 Newsletters on Stratigraphy, 45(2), 139-150, doi:10.1127/0078-0421/2012/0018.
859 Duncan, R.A., 1978. Geochronology of basalts from the Ninetyeast Ridge and continental
860 dispersion in the eastern Indian Ocean. Journal of Volcanology and Geothermal Research,
861 4, 283-305, doi:10.1016/0377-0273(78)90018-5.
862 Duncan, R.A., 1991. Age distribution of volcanism along aseismic ridges in the eastern Indian
863 Ocean. Proceedings of the Integrated Ocean Drilling Program, 121, 507-517,
864 doi:10.2973/odp.proc.sr.121.162.1991.
865 Emerson, S., and Bender, M., 1981. Carbon fluxes at the sediment-water interface of the deep-
866 sea: calcium carbonate preservation. Journal of Marine Research, 39, 139-162.
867 Eshet, Y., and Almogi-Labin, A., 1996. Calcareous nannofossils as paleoproductivity indicators
868 in Upper Cretaceous organic-rich sequences in Israel. Marine Micropaleontology, 29(1),
869 37-61, doi:10.1016/0377-8398(96)00006-0.
870 Font, E., Fabre, S., Nédélec, A., Adatte, T., Keller, G., Veiga-Pires, C., Ponte, J., Mirão, J.,
871 Khozyem, H., and Spangenberg, J.E., 2014. Atmospheric halogen and acid rains during the

872 main phase of Deccan eruptions: magnetic and mineral evidence. In: Keller, G., Kerr, A.C.
873 (Eds.), Volcanism, Impacts, and Mass Extinctions: Causes and Effects. Geological Society
874 of America Special Paper, 505, 353-368, doi:10.1130/2014.2505(18).
875 Font, E., Adatte, T., Sial, A.N., de Lacerda, L.D., Keller, G., and Punekar, J., 2016. Mercury
876 anomaly, Deccan volcanism, and the end-Cretaceous mass extinction. Geology, 44(2), 171-
877 174, doi: 10.1130/G37451.1.
878 Frank, T.D., and Arthur, M.A., 1999. Tectonic forcings of Maastrichtian ocean- climate
879 evolution. Paleoceanography, 14(2), 103-117, doi:10.1029/1998PA900017.
880 Frank, T.D., Thomas, D.J., Leckie, R.M., Arthur, M.A., Brown, P.R., Jones, K., and Lees, J.A.,
881 2005. The Maastrichtian record from Shatsky Rise (northwest Pacific): a tropical
882 perspective on global ecological and oceanographic changes. Paleoceanography, 20,
883 PA1008, doi:10.1029/2004PA001052.
884 Friedrich, O., Herrle, J.O., and Hemleben, C., 2005. Climatic changes in the Late Campanian-
885 Early Maastrichtian: Micropaleontological and stable isotopic evidence from an
886 epicontinental sea. The Journal of Foraminiferal Research, 35(3), 228-247,
887 doi:10.2113/35.3.228.
888 Friedrich, O., Schmiedl, G., and Erlenkeuser, H., 2006. Stable isotope composition of Late
889 Cretaceous benthic foraminifera from the southern South Atlantic: Biological and

environmental effects. Marine Micropaleontology, 58, 135-157, doi:10.1016/j.marmicro.2005.10.005.

Friedrich, O., Herrle, J.O., Wilson, P.A., Cooper, M.J., Erbacher, J., and Hemleben, C., 2009. Early Maastrichtian carbon cycle perturbation and cooling event: Implications from the South Atlantic Ocean. Paleoceanography, 24(2), PA2211, doi:10.1029/2008PA001654

Gardin, S., Galbrun, B., Thibault, N., Coccioni, R., and Premoli Silva, I., 2012. Biomagnetochronology for the upper Campanian–Maastrichtian from the Gubbio area, Italy: new results from the Contessa Highway and Bottaccione sections. Newsletters on Stratigraphy, 45, 75-100, doi:10.1127/0078-0421/2012/0014.

Gertsch, B., Keller, G., Adatte, T., Garg, R., Prasad, V., Fleitmann, D., and Berner, Z., 2011. Environmental effects of Deccan volcanism across the Cretaceous–Tertiary transition in Meghalaya, India. Earth and Planetary Science Letters, 310, 272-285, doi:10.1016/j.epsl.2011.08.015.

Gradstein, F.M., Ogg, J.G., Schmitz, M., and Ogg, G., 2012. The geologic time scale 2012. Boston, USA, Elsevier, pp. 1176, doi:10.1016/B978-0-444-59425-9.00004-4.

Hallock, P., 1987. Fluctuations in the trophic resource continuum: a factor in global diversity cycles? Paleoceanography, 2, 457-471, doi:10.1029/PA002i005p00457.

907 Haq, B.U., Hardenbol, J., and Vail, P.R., 1987. Chronology of fluctuating sea levels since the
908 Triassic. Science, 235(4793), 1156-1167, doi:10.1126/science.235.4793.1156.
909 Haq, B.U., 2014. Cretaceous eustasy revisited. Global and Planetary Change, 113, 44-58,
910 doi:10.1016/j.gloplacha.2013.12.007.
911 Hart, M.B., 2007. Late Cretaceous climates and foraminiferid distributions. In: Williams, M.,
912 Haywood, A.M., Gregory, F.J., Schmidt, D.N. (Eds.), Deep-Time Perspectives on Climate
913 Change: Marrying the Signal From Computer Models and Biological Proxies. Geological
914 Society Special Publication, 2, 235-250.
915 Hildebrand, A.R., Penfield, G.T., Kring, D.A., Pilkington, M., Camargo, A., Jacobsen, S.B., and
916 Boynton, W.V., 1991. Chicxulub crater: a possible Cretaceous/Tertiary boundary impact
917 crater on the Yucatan Peninsula, Mexico. Geology, 19(9), 867-871, doi:10.1130/0091-
918 7613(1991)019<0867:CCAPCT>2.3.CO;2.
919 Hönisch, B., Ridgwell, A., Schmidt, D.N., Thomas, E., Gibbs, S.J., Sluijs, A., Zeebe, R., Kump,
920 L., Martindale, R.C., Greene, S.E., Kiessling, G., Ries, J., Zachos, J.C., Royer, D.L., Barker,
921 S., Marchitto, T.M., Jr., Moyer, R., Pelejero, C., Ziveri1, P., Foster, G.L., and Williams, B.,
922 2012. The geological record of ocean acidification. Science, 335(6072), 1058-1063,
923 doi:10.1126/science.1208277.

924 Huber, B.T., Norris, R.D., and MacLeod, K.G., 2002. Deep-sea paleotemperature record of
925 extreme warmth during the Cretaceous. Geology, 30(2), 123-126, doi:10.1130/0091-
926 7613(2002)030<0123:DSPROE>2.0.CO;2.
927 Huber, B.T., MacLeod, K.G., and Tur, N.A., 2008. Chronostratigraphic framework for upper
928 Campanian-Maastrichtian sediments on the Blake Nose (subtropical North Atlantic).
929 Journal of Foraminiferal Research, 38, 162-182, doi:10.2113/gsjfr.38.2.162.
930 Husson, D., Galbrun, B., Laskar, J., Hinnov, L.A., Thibault, N., Gardin, S., and Locklair, R.E.,
931 2011. Astronomical calibration of the Maastrichtian (late Cretaceous). Earth and Planetary
932 Science Letters, 305, 328-340, doi:10.1016/j.epsl.2011.03.008.
933 Isaza-Londoño, C., MacLeod, K.G., and Huber, B.T., 2006. Maastrichtian North Atlantic
934 warming, increasing stratification, and foraminiferal paleobiology at three timescales.
935 Paleoceanography, 21, PA1012, doi:10.1029/2004PA001130.
936 Izett, G.A., 1990. The Cretaceous/Tertiary boundary interval, Raton Basin, Colorado and New
937 Mexico, and its content of shock-metamorphosed minerals; Evidence relevant to the K/T
938 boundary impact-extinction theory. Geological Society of America Special Papers, 249, 1-
939 100, doi:10.1130/SPE249-p1.
940 Keller, G., 2005. Biotic effects of late Maastrichtian mantle plume volcanism: Implications for
941 impacts and mass extinctions. Lithos, 79(3-4), 317-341, doi:10.1016/j.lithos.2004.09.005.

942 Keller, G., 2014. Deccan volcanism, the Chicxulub impact, and the end-Cretaceous mass
943 extinction: Coincidence? Cause and effect? In: Keller, G., Kerr, A.C. (Eds.), Volcanism,
944 Impacts, and Mass Extinctions: Causes and Effects. Geological Society of America Special
945 Paper, 505, 57-89, doi:10.1130/2014.2505(03).
946 Keller, G., and Abramovich, S., 2009. Lilliput effect in late Maastrichtian planktic foraminifera:
947 Response to environmental stress. Palaeogeography, Palaeoclimatology, Palaeoecology,
948 284, 47-62, doi:10.1016/j.palaeo.2009.08.029.
949 Keller, G., Adatte, T., Burns, S.J., and Tantawy, A.A., 2002. High-stress paleoenvironment
950 during the late Maastrichtian to early Paleocene in central Egypt. Palaeogeography,
951 Palaeoclimatology, Palaeoecology, 187, 35-60, doi:10.1016/S0031-0182(02)00504-7.
952 Keller, G., Bhowmick, P.K., Upadhyay, H., Dave, A., Reddy, A.N., Jaiprakash, B.C., and Adatte,
953 T., 2011. Deccan volcanism linked to the Cretaceous-Tertiary boundary (KTB) mass
954 extinction: New evidence from ONGC wells in the Krishna-Godavari Basin, India. Journal
955 of the Geological Society of India, 78, 399-428, doi:10.1007/s12594-011-0107-3.
956 Keller, G., Khozyem, H.M., Adatte, T., Malarkodi, N., Spangenberg, J.E., and Stinnesbeck, W.,
957 2013. Chicxulub Impact Spherules in the North Atlantic and Caribbean: age constraints and
958 Cretaceous-Tertiary boundary hiatus. Geological Magazine, 150(05), 885-907,
959 doi:10.1017/S0016756812001069.

960 Keller, G., Punekar, J., and Mateo, P., 2016a. Upheavals during the late Maastrichtian:
961 Volcanism, climate and faunal events preceding the end-Cretaceous mass extinction.
962 Palaeogeography, Palaeoclimatology, Palaeoecology, 441, 137-151,
963 doi:10.1016/j.palaeo.2015.06.034.
964 Keller, G., Jaiprakash, B.C., and Reddy, A.N., 2016b. Maastrichtian to Eocene subsurface
965 stratigraphy of the Cauvery basin and correlation with Madagascar. Journal of the
966 Geological Society of India, 87(1), 5-34, doi:10.1007/s12594-016-0370-4.
967 Koutsoukos, E.A.M., 1994. Early stratigraphic record and phylogeny of the planktonic genus
968 Guembelitria Cushman, 1933. Journal of Foraminiferal Research, 24, 288-295,
969 doi:10.2113/gsjfr.24.4.288.
970 Kring, D.A., 2007. The Chicxulub impact event and its environmental consequences at the
971 Cretaceous–Tertiary boundary. Palaeogeography, Palaeoclimatology, Palaeoecology,
972 255(1), 4-21, doi:10.1016/j.palaeo.2007.02.037.
973 Krishna, K.S., Abraham, H., Sager, W.W., Pringle, M.S., Frey, F., Gopala Rao, D., and
974 Levchenko, O.V., 2012. Tectonics of the Ninetyeast Ridge derived from spreading records
975 in adjacent oceanic basins and age constraints of the ridge. Journal of Geophysical
976 Research, 117, B04101, doi: 10.1029/2011JB008805.

977 Kroon, D., and Nederbragt, A.J., 1990. Ecology and paleoecology of triserial planktic
978 foraminifera. Marine Micropaleontology, 16, 25-38, doi:10.1016/0377-8398(90)90027-J.
979 Kump, L., Bralower, T., and Ridgwell, A., 2009. Ocean acidification in deep time.
980 Oceanography, 22(4), 94-107.
981 Leckie, R.M., 1987. Paleoecology of mid-Cretaceous planktonic foraminifera: a comparison of
982 open ocean and epicontinental sea assemblages. Micropaleontology, 33(2), 164-176, doi:
983 10.2307/1485491.
984 Li, L., and Keller, G., 1998a. Maastrichtian climate, productivity and faunal turnovers in planktic
985 foraminifera of South Atlantic DSDP Sites 525A and 21. Marine Micropaleontology, 33(1-
986 2), 55-86, doi:10.1016/S0377-8398(97)00027-3.
987 Li, L., and Keller, G., 1998b. Abrupt deep-sea warming at the end of the Cretaceous. Geology,
988 26, 995-998, doi:10.1130/0091-7613(1998)026<0995:ADSWAT>2.3.CO;2.
989 Li, L., and Keller, G., 1998c. Diversification and extinction in Campanian-Maastrichtian planktic
990 foraminifera of northwestern Tunisia. Eclogae Geologicae Helvetiae, 91(1), 75-102.
991 Li, L., and Keller, G., 1999. Variability in Late Cretaceous climate and deep waters: evidence
992 from stable isotopes. Marine Geology, 161, 171-190, doi:10.1016/S0025-3227(99)00078-X.

993 Li, L., Keller, G., Adatte, T., and Stinnesbeck, W., 2000. Late Cretaceous sea-level changes in
994 Tunisia: a multi-disciplinary approach. Journal of the Geological Society of London, 157,
995 447-458, doi:10.1144/jgs.157.2.447.
996 Linnert, C., Robinson, S.A., Lees, J.A., Bown, P.R., Pérez-Rodríguez, I., Petrizzo, M.R., Falzoni,
997 F., Littler, K., Arz, J.A., and Russell, E.E., 2014. Evidence for global cooling in the Late
998 Cretaceous. Nature communications, 5, 4194, doi:10.1038/ncomms5194.
999 Luyendyk, B.P., 1977. Deep Sea Drilling on the Ninetyeast Ridge: Synthesis and a Tectonic
1000 Model. In: Heirtzler, J.R., Bolli, H.M., Davies, T.A., Saunders, J.B., Sclater, J.C. (Eds.),
1001 Indian Ocean Geology and Biostratigraphy. American Geophysical Union, Washington,
1002 D.C., doi: 10.1029/SP009p0165.
1003 MacLeod, K.G., 1994. Bioturbation, inoceramid extinction, and mid-Maastrichtian ecological
1004 change. Geology, 22, 139-142, doi:10.1130/0091-7613(1994)022<0139:BIEAMM>
1005 2.3.CO;2.
1006 MacLeod, K.G., Huber, B.T., Pletsch, T., Röhl, U., and Kucera, M., 2001. Maastrichtian
1007 foraminiferal and paleoceanographic changes on Milankovitch timescales.
1008 Paleoceanography, 16(2), 133-154., doi:10.1029/2000PA000514.

1009 MacLeod, K.G., Huber, B.T., and Isaza-Londoño, C., 2005. North Atlantic warming during
1010 "global" cooling at the end of the Cretaceous. Geology, 33, 437-440,
1011 doi:10.1130/G21466.1.
1012 MacLeod, K.G., Whitney, D.L., Huber, B.T., and Koeberl, C., 2007. Impact and extinction in
1013 remarkably complete Cretaceous-Tertiary boundary sections from Demerara Rise, tropical
1014 western North Atlantic. Geological Society of America Bulletin, 119(1-2), 101-115,
1015 doi:10.1130/B25955.1.
1016 MacLeod, N., 1996. Testing patterns of Cretaceous-Tertiary planktonic foraminiferal extinction
1017 at El Kef (Tunisia). Geological Society of America Special Paper, 307, 287-302.
1018 MacLeod, N., and Keller, G., 1991. Hiatus distributions and mass extinctions at the
1019 Cretaceous/Tertiary boundary. Geology, 19, 497-501, doi: 10.1130/0091-
1020 7613(1991)019b0497:HDAMEAN2.3.CO;2.
1021 MacLeod, N., Ortiz, N., Fefferman, N., Clyde, W., Schulter, C., and MacLean, J., 2000.
1022 Phenotypic response of foraminifera to episodes of global environmental change. In:
1023 Culver, S.J., Rawson, P. (Eds.), Biotic Response to Global Environmental Change: The
1024 Last 145 Million Years. Cambridge, UK, Cambridge University Press, pp. 51-78.

1025 Malmgren, B.A., 1987. Differential dissolution of Upper Cretaceous planktonic foraminifera
1026 from a temperate region of the South Atlantic Ocean. Marine Micropaleontology, 11(4),
1027 251-271, doi:10.1016/0377-8398(87)90001-6.
1028 Mateo, P., Keller, G., Adatte, T., and Spangenberg, J.E., 2016. Mass wasting and hiatuses during
1029 the Cretaceous-Tertiary transition in the North Atlantic: Relationship to the Chicxulub
1030 impact? Palaeogeography, Palaeoclimatology, Palaeoecology, 441, 96-115,
1031 doi:10.1016/j.palaeo.2015.01.019.
1032 Meilijson, A., Ashckenazi-Polivoda, S., Ron-Yankovich, L., Illner, P., Alsenz, H., Speijer, R.P.,
1033 Almogi-Labin, A., Feinstein, S., Berner, Z., Püttmann, W., and Abramovich, S., 2014.
1034 Chronostratigraphy of the Upper Cretaceous high productivity sequence of the southern
1035 Tethys, Israel. Cretaceous Research, 50, 187-213, doi:10.1016/j.cretres.2014.04.006.
1036 Moore, D.G., Curray, J.R., Raitt, R.W., and Emmel, F.J., 1974. Stratigraphic-seismic sections
1037 correlations and implications to Bengal fan history. In: von der Borch, C.C., Slater, J.G., et
1038 al. (Eds.), Initial Reports of the Deep Sea Drilling Project, 22. U.S. Government Printing
1039 Office, Washington, pp. 403-412, doi:10.2973/dsdp.proc.22.116.1974.
1040 Moy, A.D., Howard, W.R., Bray, S.G., and Trull, T.W., 2009. Reduced calcification in modern
1041 Southern Ocean planktonic foraminifera. Nature Geoscience, 2(4), 276-280,
1042 doi:10.1038/ngeo460.

1043 Nederbragt, A.J., 1991. Late Cretaceous biostratigraphy and development of Heterohelicidae
1044 (planktic foraminifera). Micropaleontology, 37(4), 329-372, doi:10.2307/1485910.
1045 Nordt, L., Atchley, S., and Dworkin, S., 2003. Terrestrial evidence for two greenhouse events in
1046 the latest Cretaceous. GSA Today, 13(12), 4-9, doi:10.1130/1052-
1047 5173(2003)013<4:TEFTGE>2.0.CO;2.
1048 Norris, R.D., Huber, B.T., and Self-Trail, J., 1999. Synchroneity of the KT oceanic mass
1049 extinction and meteorite impact: Blake Nose, western North Atlantic. Geology, 27(5), 419-
1050 22, doi:10.1130/0091-7613(1999)027<0419:SOTKTO>2.3.CO;2.
1051 Olsson, R.K., Miller, K.G., Browning, J.V., Habib, D., and Sugarmann, P.J., 1997. Ejecta layer
1052 at the Cretaceous-Tertiary boundary, Bass River, New Jersey (Ocean Drilling Program Leg
1053 174AX). Geology, 25(8), 759-62, doi:10.1130/0091-
1054 7613(1997)025<0759:ELATCT>2.3.CO;2.
1055 Olsson, R.K., Hemleben, C., Berggren, W.A., and Huber, B.T., 1999. Atlas of Paleocene
1056 Planktonic Foraminifera. Smithsonian Contributions to Paleobiology, 85. Washington, DC,
1057 Smithsonian Institution Press, pp. 252.
1058 Olsson, R.K., Wright, J.D., and Miller, K.G., 2001. Paleobiogeography of *Pseudotextularia*
1059 *elegans* during the latest Maastrichtian global warming event. Journal of Foraminiferal
1060 Research, 31, 275-282, doi:10.2113/31.3.275.

1061 Pardo, A., and Keller, G., 2008. Biotic effects of environmental catastrophes at the end of the
1062 Cretaceous: Guembelitria and Heterohelix blooms. Cretaceous Research, 29(5-6), 1058-
1063 1073, doi:10.1016/j.cretres.2008.05.031.
1064 Parker, F.L., and Berger, W.H., 1971. Faunal and solution patterns of planktonic foraminifera in
1065 surface sediments of the South Pacific. Deep Sea Research and Oceanographic Abstracts,
1066 18(1), 73-107, doi:10.1016/0011-7471(71)90017-9.
1067 Premoli Silva, I., and Sliter, W.V., 1999. Cretaceous paleoceanography: evidence from
1068 planktonic foraminiferal evolution. Special Papers-Geological Society of America, 301-328.
1069 Pringle, M.S., Frey, F.A., and Mervine, E.M., 2008. A simple linear age progression for the
1070 Ninetyeast Ridge, Indian Ocean: new constraints on Indian plate tectonics and hotspot
1071 dynamics. Eos Transactions AGU Fall Meeting Supplementary Abstract 89, p. T54B-03.
1072 Punekar, J., Mateo, P., and Keller, G., 2014a. Effects of Deccan volcanism on paleoenvironment
1073 and planktic foraminifera: A global survey. In: Keller, G., Kerr, A.C. (Eds.), Volcanism,
1074 Impacts, and Mass Extinctions: Causes and Effects. Geological Society of America Special
1075 Paper, 505, 91-116, doi: 10.1130/2014.2505(04).
1076 Punekar, J., Keller, G., Khozyem, H.M., Hamming, C., Adatte, T., Tantawy, A.A., and
1077 Spangenberg, J., 2014b. Late Maastrichtian-early Danian high-stress environments and

1078 delayed recovery linked to Deccan volcanism. Cretaceous Research, 49, 63-82.
1079 doi:10.1016/j.cretres.2014.01.002.
1080 Punekar, J., Keller, G., Khozyem, H. M., Adatte, T., Font, E., and Spangenberg, J., 2016. A
1081 multi-proxy approach to decode the end-Cretaceous mass extinction. Palaeogeography,
1082 Palaeoclimatology, Palaeoecology, 441, 116-136, doi:10.1016/j.palaeo.2015.08.025.
1083 Renne, P.R., Sprain, C.J., Richards, M.A., Self, S., Vanderkluysen, L., and Pande, K., 2015.
1084 State shift in Deccan volcanism at the Cretaceous-Paleogene boundary, possibly induced
1085 by impact. Science, 350(6256), 76-78, doi:10.1126/science.aac7549.
1086 Richards, M.A., Alvarez, W., Self, S., Karlstrom, L., Renne, P.R., Manga, M., Sprain, C.J., Smit,
1087 J., Vanderkluysen, L., and Gibson, S.A., 2015. Triggering of the largest Deccan eruptions
1088 by the Chicxulub impact. Geological Society of America Bulletin, 127(11-12), 1507-1520,
1089 doi:10.1130/B31167.1.
1090 Robaszynski, F., Caron, M., Gonzalez Donoso, J.M., and Wonders, A.A.H., 1983-1984. Atlas of
1091 Late Cretaceous globotruncanids. Micropaleontology, 26(3-4), 145-305.
1092 Rocchia, R., Robin, E., Froget, L., and Gayraud, J., 1996. Stratigraphic distribution of
1093 extraterrestrial markers at the Cretaceous–Tertiary boundary in the Gulf of Mexico area:
1094 Implications for the temporal complexity of the event. In: Ryder, G., Fastovsky, D.,

Gartner, S. (Eds.), The Cretaceous-Tertiary event and other catastrophes in Earth History. Geological Society of America, Special Papers, 307, 279-286.

Schöbel, S., deWall, H., Ganerød,M., Pandit,M.K., and Rolf, C., 2014. Magnetostratigraphy and 40Ar–39Ar geochronology of the Malwa Plateau region (Northern Deccan Traps), central western India: significance and correlation with the main Deccan Large Igneous Province sequences. Journal of Asian Earth Sciences, 89, 28-45, doi:10.1016/j.jseaes.2014.03.022.

Schoene, B., Samperton, K.M., Eddy, M.P., Keller, G., Adatte, T., Bowring, S.A., Khadri, S.F.R., and Gertsch, B., 2015. U–Pb geochronology of the Deccan Traps and relation to the end-Cretaceous mass extinction. Science, 347, 182-184, doi:10.1126/science.aaa0118.

Schrag, D.P., DePaolo, D.J., and Richter, F.M., 1995. Reconstructing past sea surface temperatures from oxygen isotope measurements of bulk carbonate. Geochimica et Cosmochimica Acta, 59, 2265-2278, doi:10.1016/0016-7037(95)00105-9.

Schultz, P.H., and D'Hondt, S., 1996. Cretaceous-Tertiary (Chicxulub) impact angle and its consequences. Geology, 24(11), 963-967; doi:10.1130/0091-7613(1996)024<0963:CTCIAA>2.3.CO;2.

Sclater, J.G., and Fisher, R.L., 1974. Evolution of the East Central Indian Ocean, with Emphasis on the Tectonic Setting of the Ninetyeast Ridge. Geological Society of America Bulletin, 85(5), 683-702, doi:10.1130/0016-7606(1974)85<683:EOTECI>2.0.CO;2.

1113 Scotese, C.R., 2013. Map Folio 16, KT Boundary (65.5 Ma, latest Maastrichtian), PALEOMAP
1114 PaleoAtlas for ArcGIS, volume 2, Cretaceous, PALEOMAP Project, Evanston, IL.
1115 Self, S., Jay, A.E., Widdowson, M., and Keszthelyi, L.P., 2008. Correlation of the Deccan and
1116 Rajahmundry Trap lavas: Are these the longest and largest lava flows on Earth? Journal of
1117 Volcanology and Geothermal Research, 172, 3-19, doi:10.1016/j.jvolgeores.2006.11.012.
1118 Shackleton, N.J., 1987. Oxygen isotopes, ice volume and sea level. Quaternary Science Reviews,
1119 6(3-4), 183-190, doi:10.1016/0277-3791(87)90003-5.
1120 Smit, J., 1999. The global stratigraphy of the Cretaceous/Tertiary boundary impact ejecta.
1121 Annual Review of Earth and Planetary Sciences, 27, 75-91,
1122 doi:10.1146/annurev.earth.27.1.75.
1123 Smit, J., Montanari, A., Swinburne, N.H.M., Alvarez, W., Hildebrand, A.R., Margolis, S.V.,
1124 Claeys, P., Lowrie, W., and Asaro, F., 1992. Tektite-bearing, deep-water clastic unit at the
1125 Cretaceous-Tertiary boundary in northeastern Mexico. Geology, 20, 99-103.
1126 Smit, J., Roep, T.B., Alvarez, W., Montanari, A., Claeys, P., Grajalesnishimura, J.M., and
1127 Bermudez, J., l996. Coarse-grained clastic sandstone complex at the K/T boundary around
1128 the Gulf of Mexico: Deposition by tsunami waves induced by the Chicxulub impact? In:
1129 Ryder, G., Fastovsky, D., Gartner, S. (Eds.), The Cretaceous-Tertiary Event and other

1130 Catastrophes in Earth History. Geological Society of America Special Paper, 307, 151-182,
1131 doi:10.1130/0-8137-2307-8.151.
1132 Stüben, D., Kramar, U., Harting, M., Stinnesbeck, W., and Keller, G., 2005. High-resolution
1133 geochemical record of Cretaceous-Tertiary boundary sections in Mexico: New constraints
1134 on the K/T and Chicxulub events. Geochimica et Cosmochimica Acta, 69(10), 2559-2579,
1135 doi:10.1016/j.gca.2004.11.003.
1136 Tantawy, A.A., Keller, G., and Pardo, A., 2009. Late Maastrichtian volcanism in the Indian
1137 Ocean: effects on calcareous nannofossils and planktic foraminifera. Palaeogeography,
1138 Palaeoclimatology, Palaeoecology, 284, 63-87, doi:10.1016/j.palaeo.2009.08.025.
1139 Thibault, N., 2016. Calcareous nannofossil biostratigraphy and turnover dynamics in the late
1140 Campanian–Maastrichtian of the tropical South Atlantic. Revue de Micropaléontologie,
1141 59(1), 57-69, doi:10.1016/j.revmic.2016.01.001.
1142 Thibault, N., and Gardin, S., 2007. The late Maastrichtian nannofossil record of climate change
1143 in the South Atlantic DSDP Hole 525A. Marine Micropaleontology, 65, 163–184,
1144 doi:10.1016/j.marmicro.2007.07.004.
1145 Thibault, N., and Gardin, S., 2010. The calcareous nannofossil response to the end-Cretaceous
1146 warm event in the Tropical Pacific. Palaeogeography, Palaeoclimatology, Palaeoecology,
1147 291, 239-252, doi: 10.1016/j.palaeo.2010.02.036.

1148 Thibault, N., and Husson, D., 2016. Climatic fluctuations and sea-surface water circulation
1149 patterns at the end of the Cretaceous era: Calcareous nannofossil evidence.
1150 Palaeogeography, Palaeoclimatology, Palaeoecology, 441, 152-164,
1151 doi:10.1016/j.palaeo.2015.07.049.
1152 Thompson, G., Bryan, W.B., Frey, F.A., and Sung, A.C., 1974. Petrology and geochemistry of
1153 basalts and related rocks from sites 214, 215, 217 DSDP Leg 22, Indian Ocean In: von der
1154 Borch, C.C., Slater, J.G., et al. (Eds.), Initial Reports of the Deep Sea Drilling Project, 22.
1155 U.S. Government Printing Office, Washington, pp. 459-468,
1156 doi:10.2973/dsdp.proc.22.119.1974.
1157 Thunell, R.C., 1976. Optimum indices of calcium carbonate dissolution, in deep-sea sediments.
1158 Geology, 4(9), 525-528, doi: 10.1130/0091-7613(1976)4<525:OIOCCD>2.0.CO;2.
1159 Tobin T.S., Ward P.D., Steig E.J., Olivero E.B., Hilburn I.A., Mitchell R.N., Diamond M.R.,
1160 Raub T.D., and Kirschvink J.L., 2012. Extinction patterns, $\delta^{18}O$ trends, and
1161 magnetostratigraphy from a southern high-latitude Cretaceous–Paleogene section: Links
1162 with Deccan volcanism. Palaeogeography, Palaeoclimatology, Palaeoecology, 350-352,
1163 180-188, doi:10.1016/j.palaeo.2012.06.029.

1164 Tsujita, C.J., 2001. The significance of multiple causes and coincidence in the geological record:
1165 from clam clusters to Cretaceous catastrophe. Canadian Journal of Earth Sciences, 38(2),
1166 271-292, doi:10.1139/e00-048.
1167 Vellekoop, J., Sluijs, A., Smit, J., Schouten, S., Weijers, J.W., Damsté, J.S.S., and Brinkhuis, H.,
1168 2014. Rapid short-term cooling following the Chicxulub impact at the Cretaceous–
1169 Paleogene boundary. Proceedings of the National Academy of Sciences, 111(21), 7537-
1170 7541, doi:10.1073/pnas.1319253111.
1171 Vermeij, G.J., 1995. Economics, volcanoes, and Phanerozoic revolutions. Paleobiology, 21(02),
1172 125-152, doi:10.1017/S0094837300013178.
1173 Vincent, E., and Berger, W.H., 1985. Carbon dioxide and polar cooling in the Miocene: The
1174 Monterey hypothesis. In: Sundquist, E.T., Broecker, W.S. (Eds.), The Carbon Cycle and
1175 Atmospheric CO: Natural Variations Archean to Present. American Geophysical Union,
1176 Washington, D.C., pp. 455-468, doi:10.1029/GM032p0455.
1177 Von der Borch, C.C., Sclater, J. G., Gartner Jr., S., Hekinian, R., Johnson, D.A., McGowran, B.,
1178 Pimm, A.C., Thompson, R.W., Veevers, J.J., and Waterman, L.S., 1974. Site 217. Initial
1179 Reports of the Deep Sea Drilling Project, 22. U.S. Government Printing Office,
1180 Washington, pp. 267-324, doi:10.2973/dsdp.proc.22.108.1974.

1181 Wignall, P.B., 2001. Large igneous provinces and mass extinctions. Earth-Science Reviews,
1182 53(1-2), 1-33, doi:10.1016/S0012-8252(00)00037-4.
1183 Wilf, P., Johnson, K.R., and Huber, B.T., 2003. Correlated terrestrial and marine evidence for
1184 global climate changes before mass extinction at the Cretaceous-Paleogene boundary.
1185 Proceedings of the National Academy of Sciences of the United States of America, 100(2),
1186 599-604, doi:10.1073/pnas.0234701100.
1187 Williams, D.F., Healy-Williams, N., and Laschak, P., 1985. Dissolution and water-mass patterns
1188 in the southeast Indian Ocean, Part I: Evidence from Recent to late Holocene foraminiferal
1189 assemblages. Geological Society of America Bulletin, 96(2), 176-189, doi:10.1130/0016-
1190 7606(1985)96<176:DAWPIT>2.0.CO;2.
1191 Zachos, J.C., Arthur, M.A., and Dean, W.E., 1989. Geochemical evidence for suppression of
1192 pelagic marine productivity at the Cretaceous/Tertiary boundary. Nature, 337, 61- 64.
1193 Zachos, J.C., Lohmann, K.C., Walker, J.C., and Wise, S.W., 1993. Abrupt climate change and
1194 transient climates during the Paleogene: A marine perspective. The Journal of Geology,
1195 101(2), 191-213.
1196 Zepeda, M.A., 1998. Planktonic foraminiferal diversity, equitability and biostratigraphy of the
1197 uppermost Campanian-Maastrichtian, ODP leg 122, hole 762C, Exmouth Plateau, NW

1198 Australia, eastern Indian ocean. Cretaceous Research, 19(2), 117-152,
1199 doi:10.1006/cres.1997.0097.

FIGURE CAPTIONS

Figure 1: Paleolocation (66 Ma) of Maastrichtian sections, Reunion and Kerguelen hotspots and Deccan volcanism discussed in this study. Paleomap from Scotese (2013).

Figure 2: Maastrichtian-early Paleocene biostratigraphy for planktic foraminifera is based on the zonation scheme of Keller et al. (2002) and Li and Keller (1998a) and plotted against the magnetic polarity time scale of Site 525A. Other zonal schemes are shown for comparison. Note the overall correlation of hiatuses and sea-level events, particularly the increased number of erosion events beginning in C30n, correlative with the onset of Deccan volcanism, reflecting increased climate variability, intensified currents and erosion.

Figure 3: Maastrichtian biostratigraphy and relative species abundances of planktic foraminifera (>150 μm size fraction) at Ninety East Ridge DSDP Site 217, Indian Ocean.

Figure 4: Maastrichtian biostratigraphy and relative species abundances of planktic foraminifera (63-150 μm size fraction) at Ninety East Ridge DSDP Site 217, Indian Ocean. Note increased

1217 abundance of *Guembelitria cretacea* in zone CF3 (dark purple) and abundance peaks in the 38-
1218 63 μm size fraction (light purple), indicating increasingly high-stress environments in zone CF3.
1219
1220 Figure 5: Maastrichtian stable isotopic data of benthic foraminifera (*Gavelinella beccariformis*
1221 and *Cibicidoides* species) recording climate and productivity changes in bottom waters at Ninety
1222 East Ridge DSDP Site 217, Indian Ocean, as compared with South Atlantic DSDP Site 525A (Li
1223 and Keller, 1998a). Note the warm-cool transition in CF4 (from low to high $\delta^{18}O$ values). The
1224 low-resolution record at Site 525A (Li and Keller; 1998a) is consistent with high-resolution
1225 records by Li and Keller (1998b) and Friedrich et al. (2009).
1226
1227 Figure 6: Biostratigraphy of Maastrichtian planktic foraminifera at Ninety East Ridge DSDP Site
1228 217, Indian Ocean. Species ranges based on composite occurrences in the >150 μm and 63-150
1229 μm size fractions. Index species marked in red. Note rapid species originations in zones CF8-
1230 CF6 and a minor extinction event in zone CF4.
1231
1232 Figure 7: Biostratigraphy of Maastrichtian planktic foraminifera in Kali-H well, Cauvery Basin,
1233 India (Keller et al., 2016b; this study). Index species marked in red. Note rapid species
1234 originations in zones CF8-CF6 and a minor extinction event in zone CF4.

Figure 8: Biostratigraphy of Maastrichtian planktic foraminifera at Elles and El Kef, Tunisia (Li and Keller, 1998c; Abramovich and Keller, 2002). Note rapid species originations in zones CF8-CF6 and a minor extinction event in zone CF5.

Figure 9: Biostratigraphy of Maastrichtian planktic foraminifera at DSDP Site 525A, South Atlantic Ocean (Li and Keller, 1998a). Note rapid species originations in zones CF8-CF6 and a minor extinction event in zone CF4.

Figure 10: Maastrichtian ecological associations of planktic foraminifera (63-150 μm size fraction) at Ninety East Ridge DSDP Site 217, Indian Ocean. Note increased abundance of the opportunist *Guembelitria* species (purple) and the generalist *Globotruncanella* species (green) in zone CF3 indicating increasingly high-stress environments and dwarfing.

Figure 11: A) Maastrichtian ecological associations and B) depth ranking of planktic foraminifera (>150 μm size fraction) at Ninety East Ridge DSDP Site 217, Indian Ocean. Note increased abundance of surface and deep dwelling species in zone CF3 indicating reduced water

mass stratification. Depth ranking based on oxygen and carbon stable isotopes (Abramovich et al., 2003, 2011; Ashkenazi-Polivoda et al., 2014).

Figure 12: Maastrichtian stable isotopic data of benthic foraminifera (*Gavelinella beccariformis* and *Cibicidoides* species), species richness, dwarfing, planktic/benthic foraminiferal ratio (63-150 μm) and fragmentation index in Ninety East Ridge DSDP Site 217, Indian Ocean. Note increased dwarfing, increased abundance of benthic foraminifera and increased fragmentation in zone CF3 indicating increasingly high-stress environments and dissolution.

Figure 13: Late Campanian-Maastrichtian climate, productivity and diversity changes based on planktic foraminifera at the South Atlantic DSDP Site 525A compared with species diversity from the Tethys (El Kef and Elles, Tunisia) and Indian Ocean (Site 217, Cauvery Basin). Four climatic and faunal events lead up to the K/T mass extinction revealing major upheavals in planktic foraminifera during the last 5 Myr of the Maastrichtian.

TABLE CAPTIONS

Table 1: Maastrichtian planktic foraminiferal species census data summary at DSDP Site 217, Cauvery Basin well Kali-H, India (Keller et al., 2016b), El Kef and Elles, Tunisia (Li and Keller, 1998c; Abramovich and Keller, 2002), and DSDP Site 525A (Li and Keller, 1998a). Note: N° of species per zone represent averages; some species may have been grouped or not recognized because of rarity, which may account for some variation in species richness. *Species that originate during the CF8a-CF5 diversification event (based on the complete records of Elles and Site 525A) but are not recorded, as the recovery of zone CF8a is incomplete.

Figure 1

Click here to download high resolution image

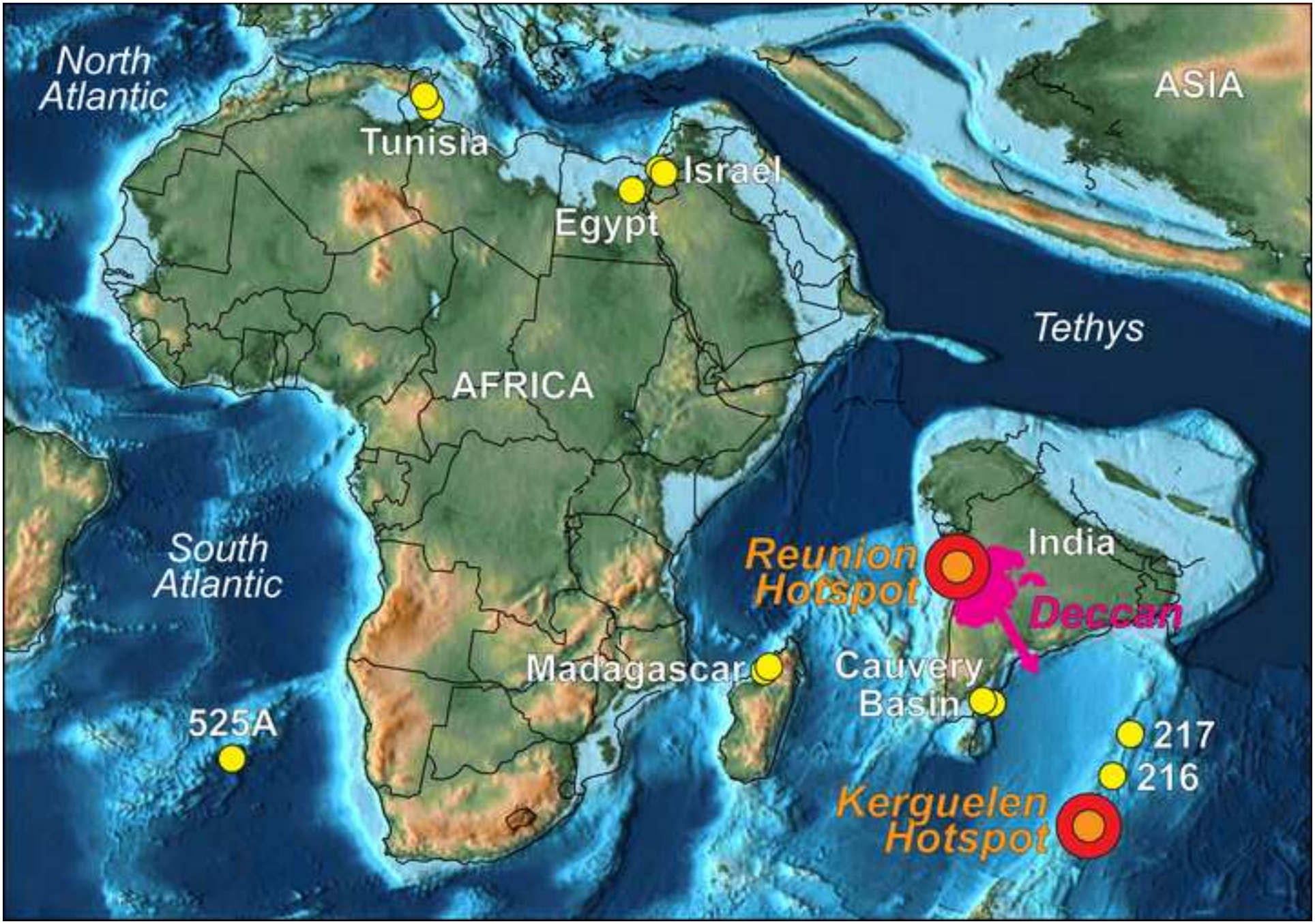

Figure 2

Click here to download high resolution image

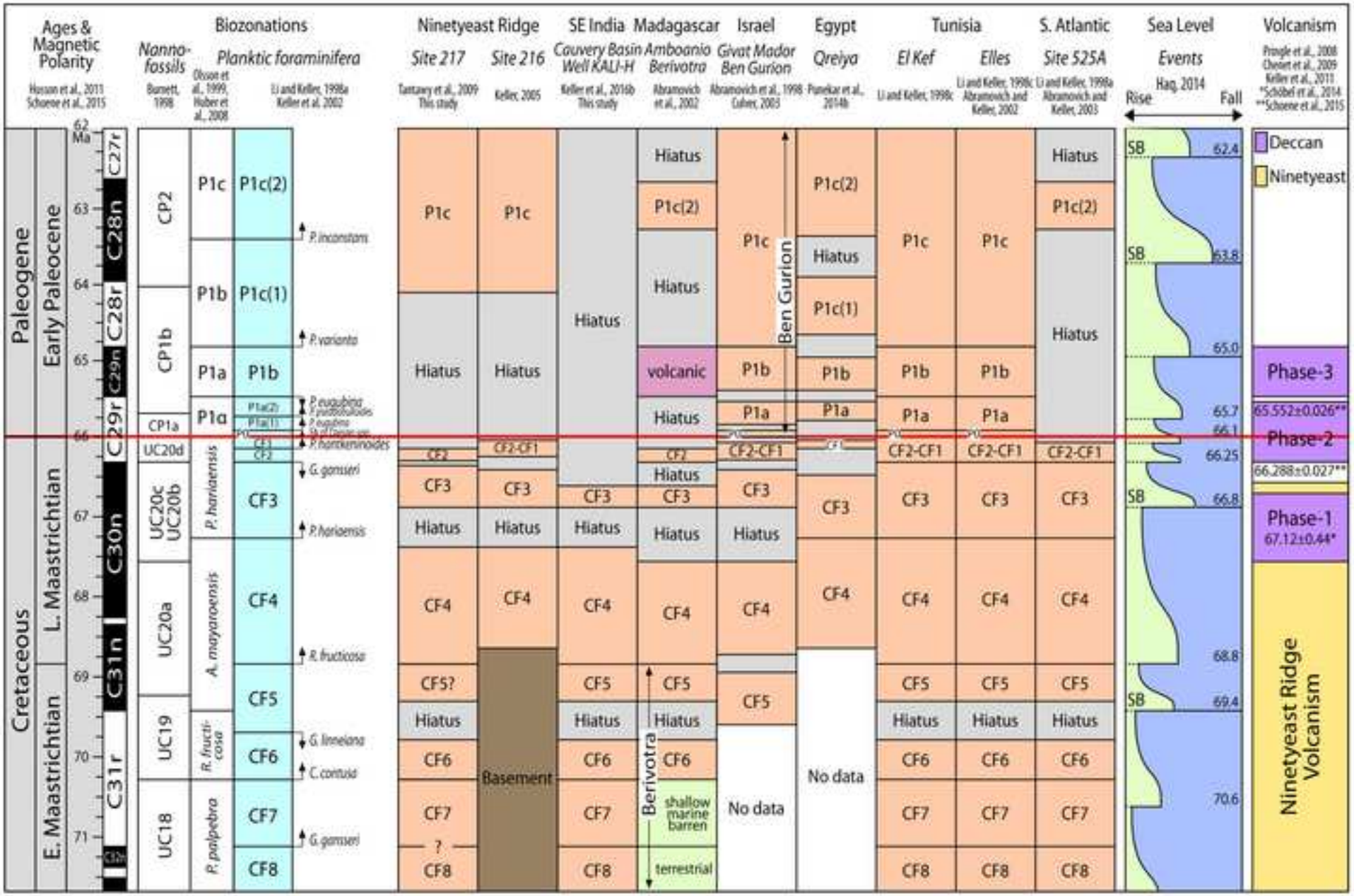

Figure 3

Click here to download high resolution image

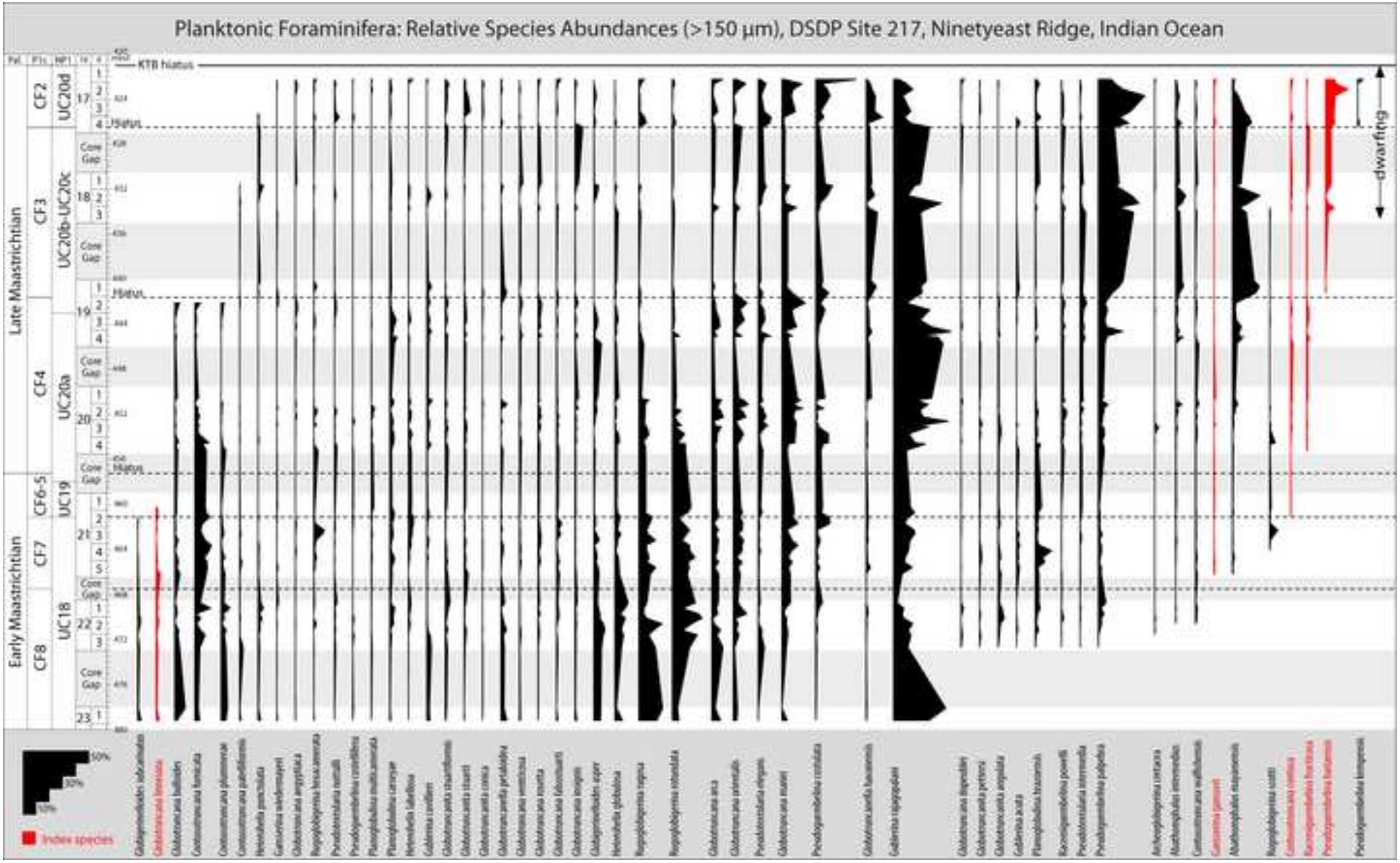

Figure 4

Click here to download high resolution image

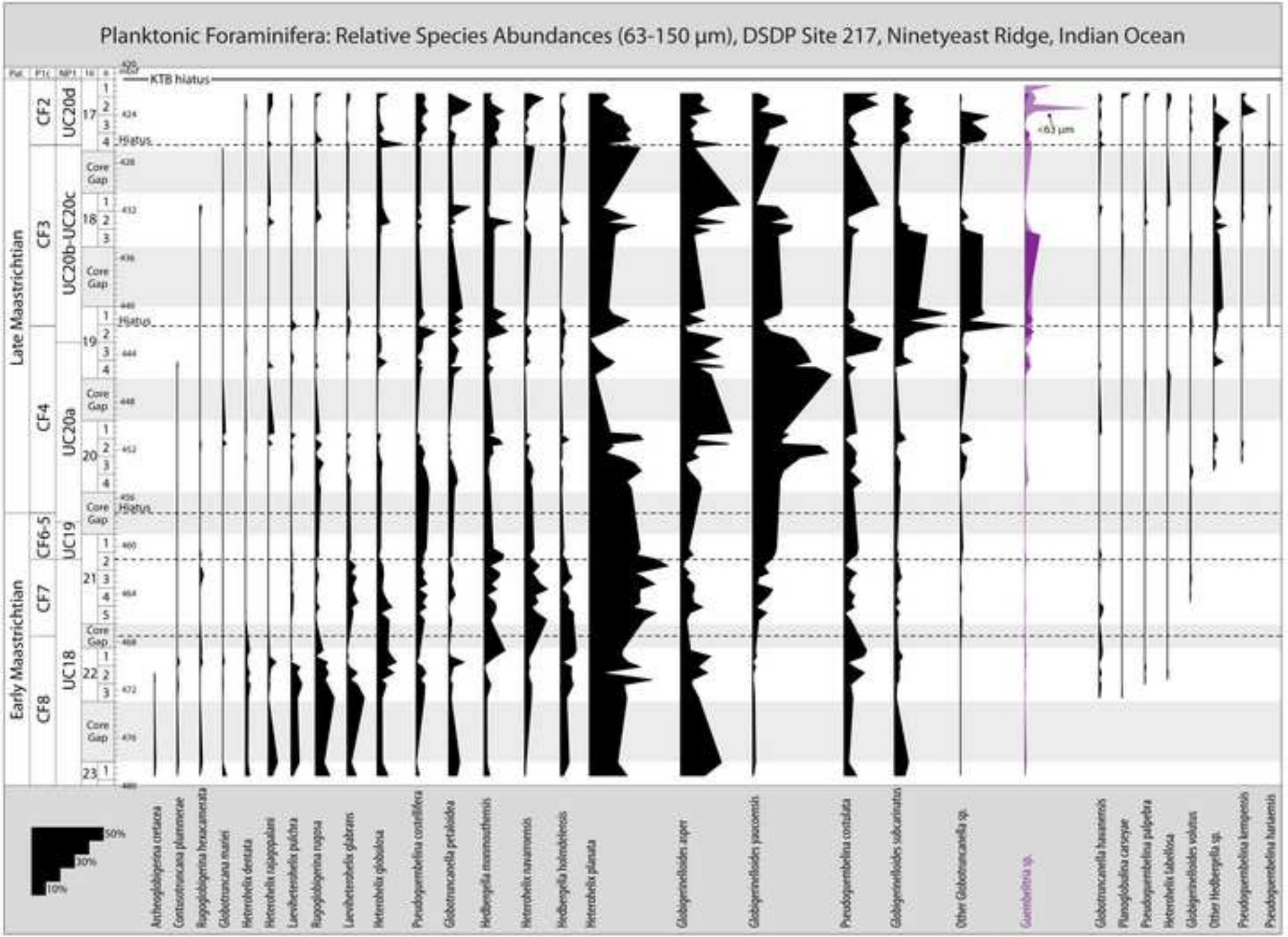

Figure 5

Click here to download high resolution image

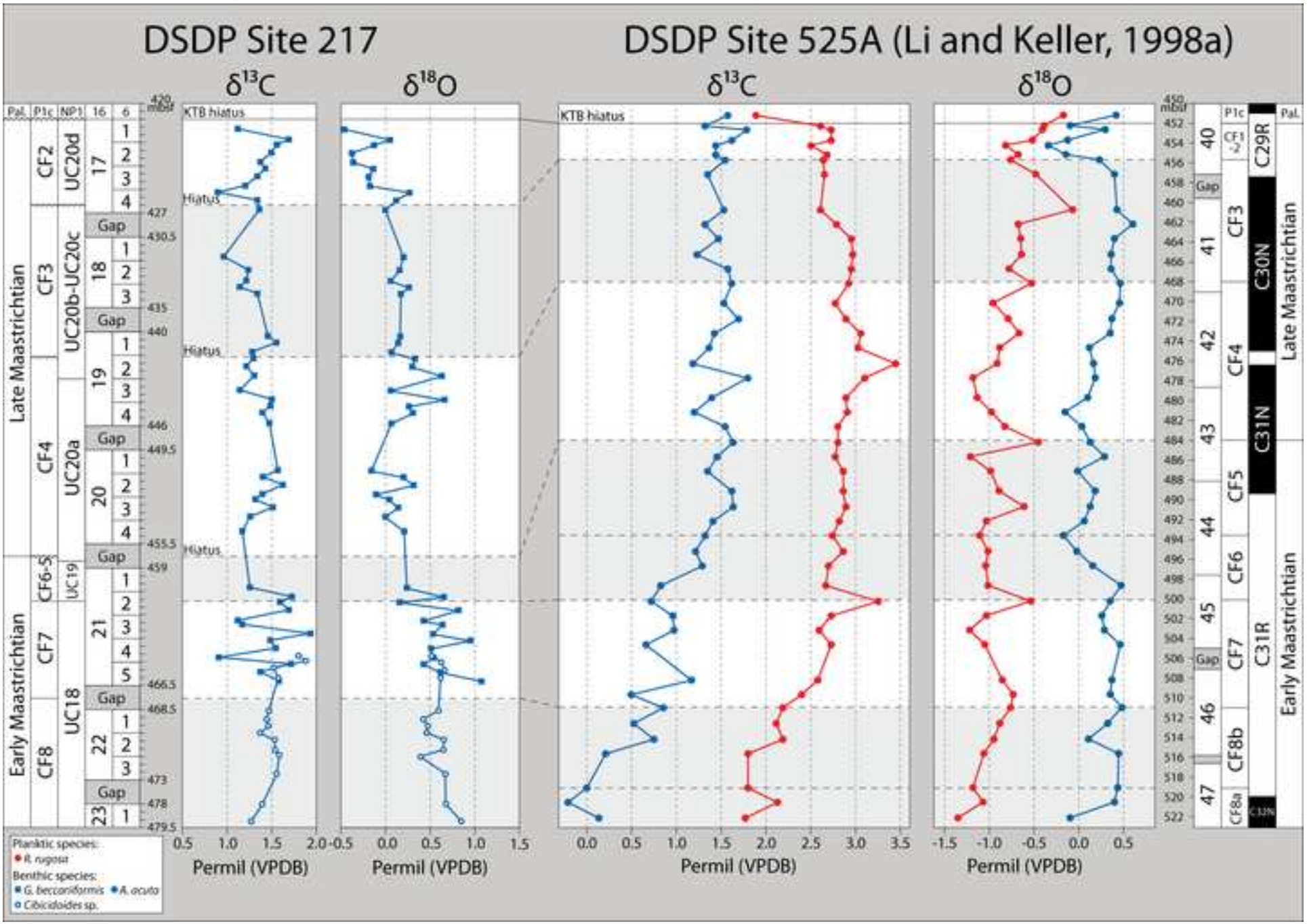

Figure 6

Click here to download high resolution image

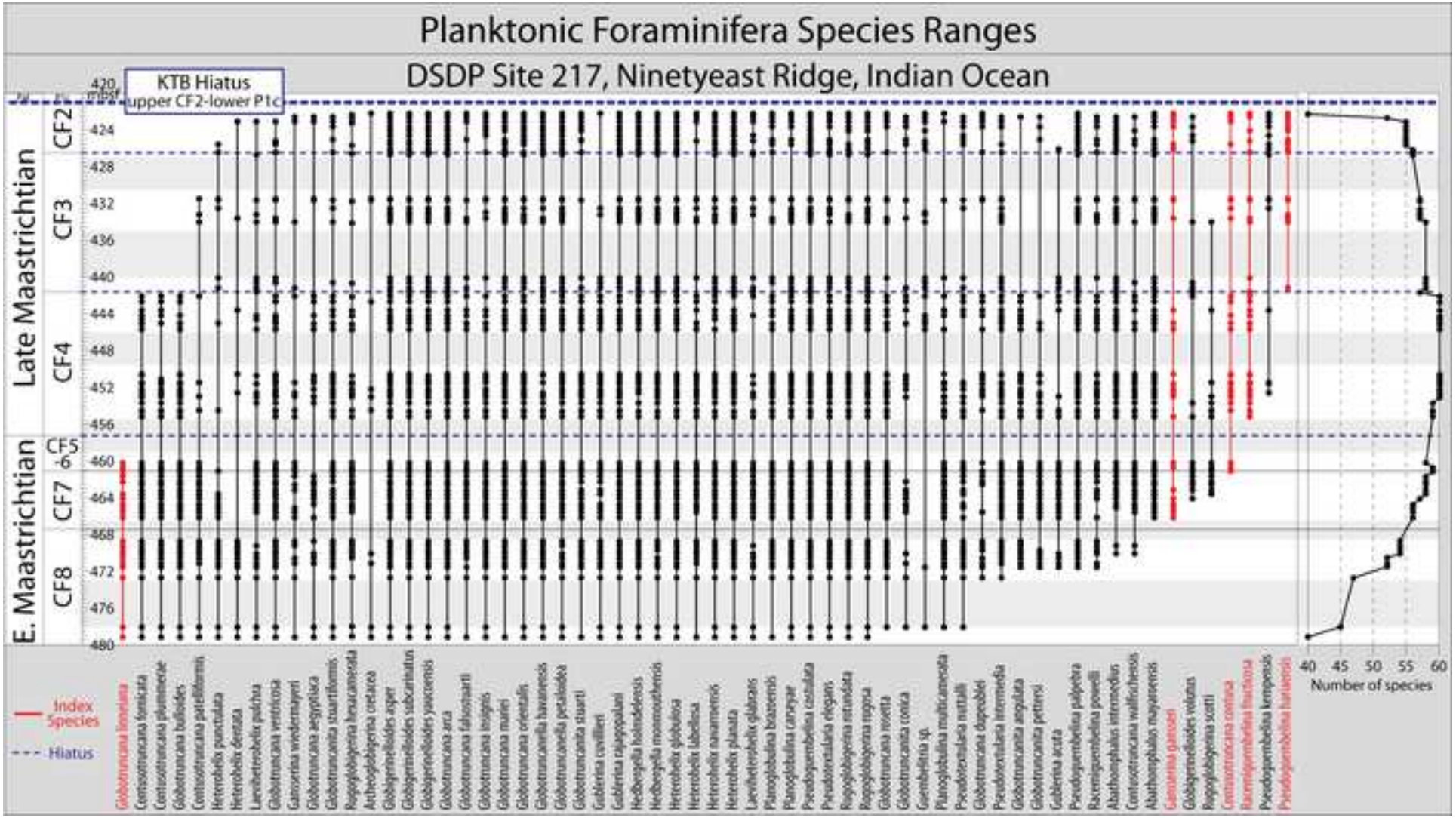

Figure 7

Click here to download high resolution image

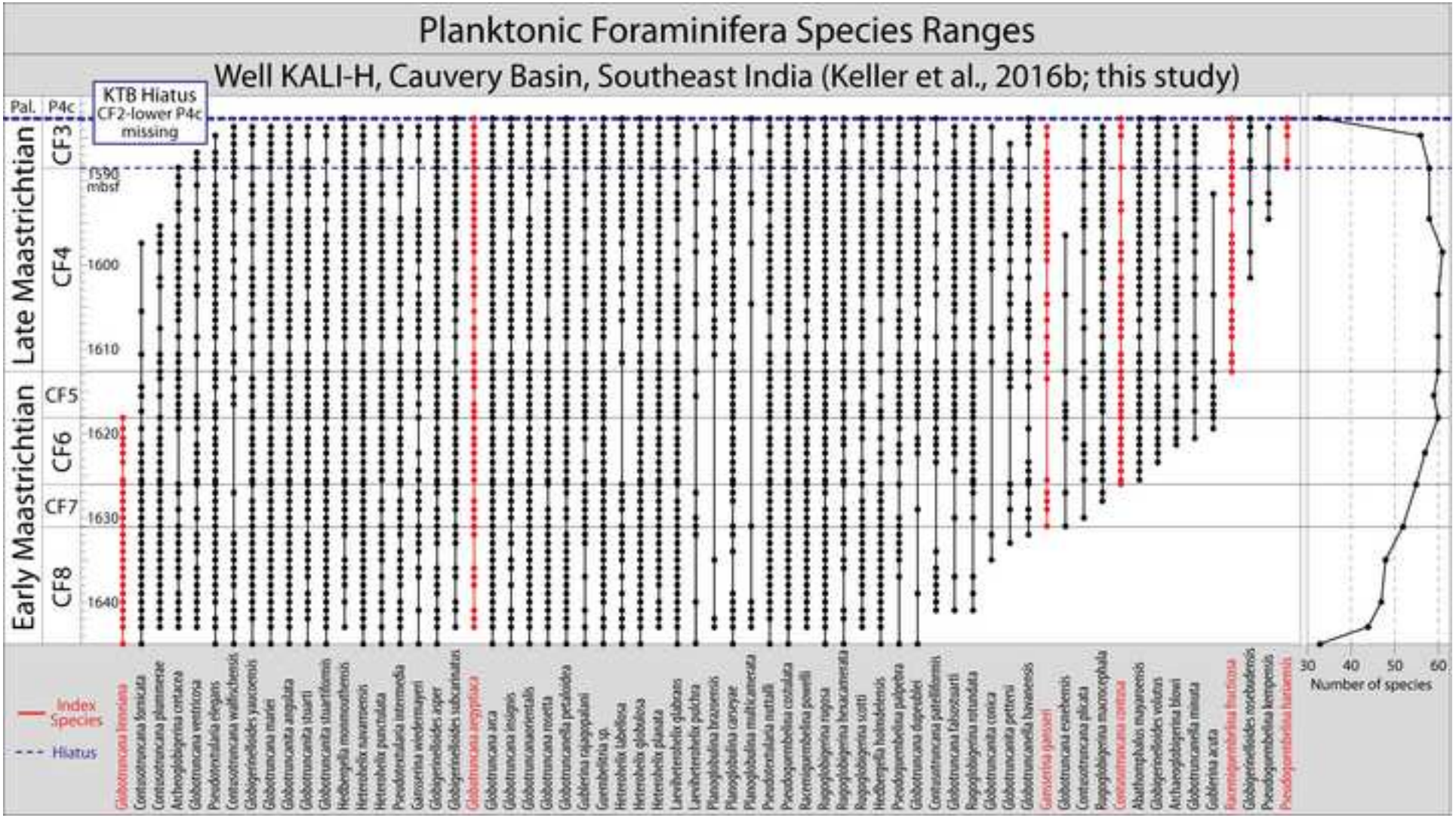

Figure 8

Click here to download high resolution image

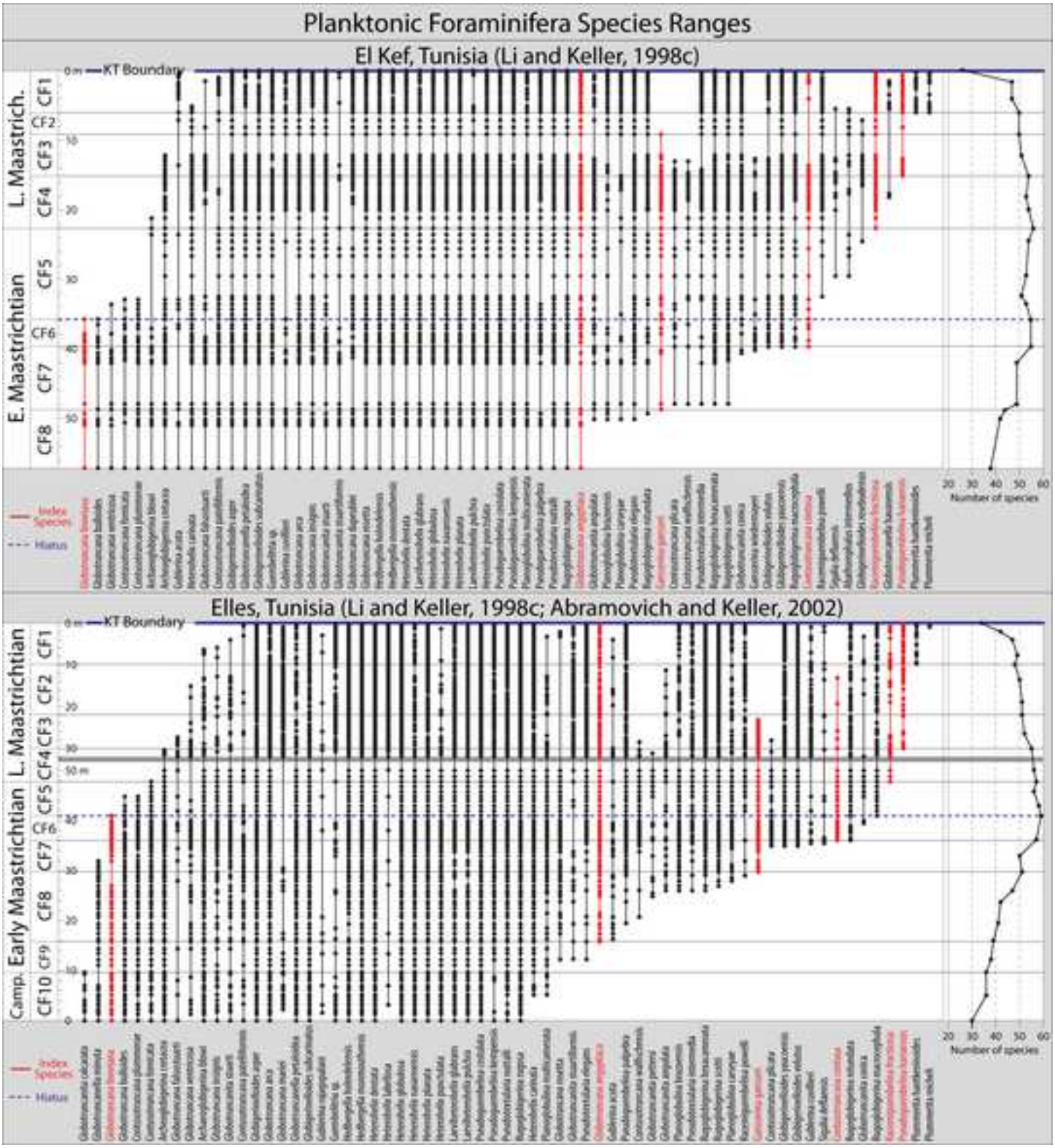

Figure 9

Click here to download high resolution image

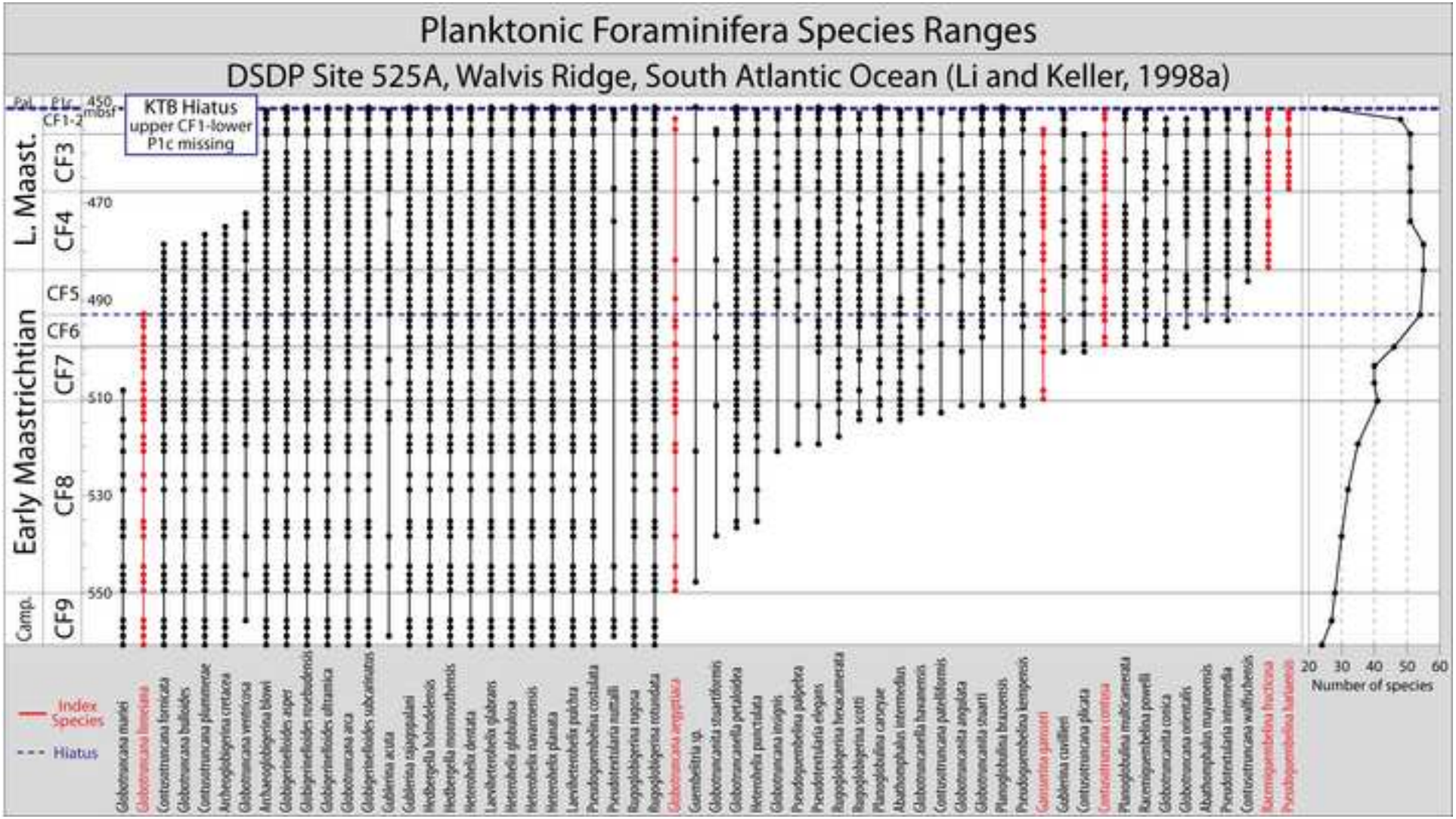

Figure 10

Click here to download high resolution image

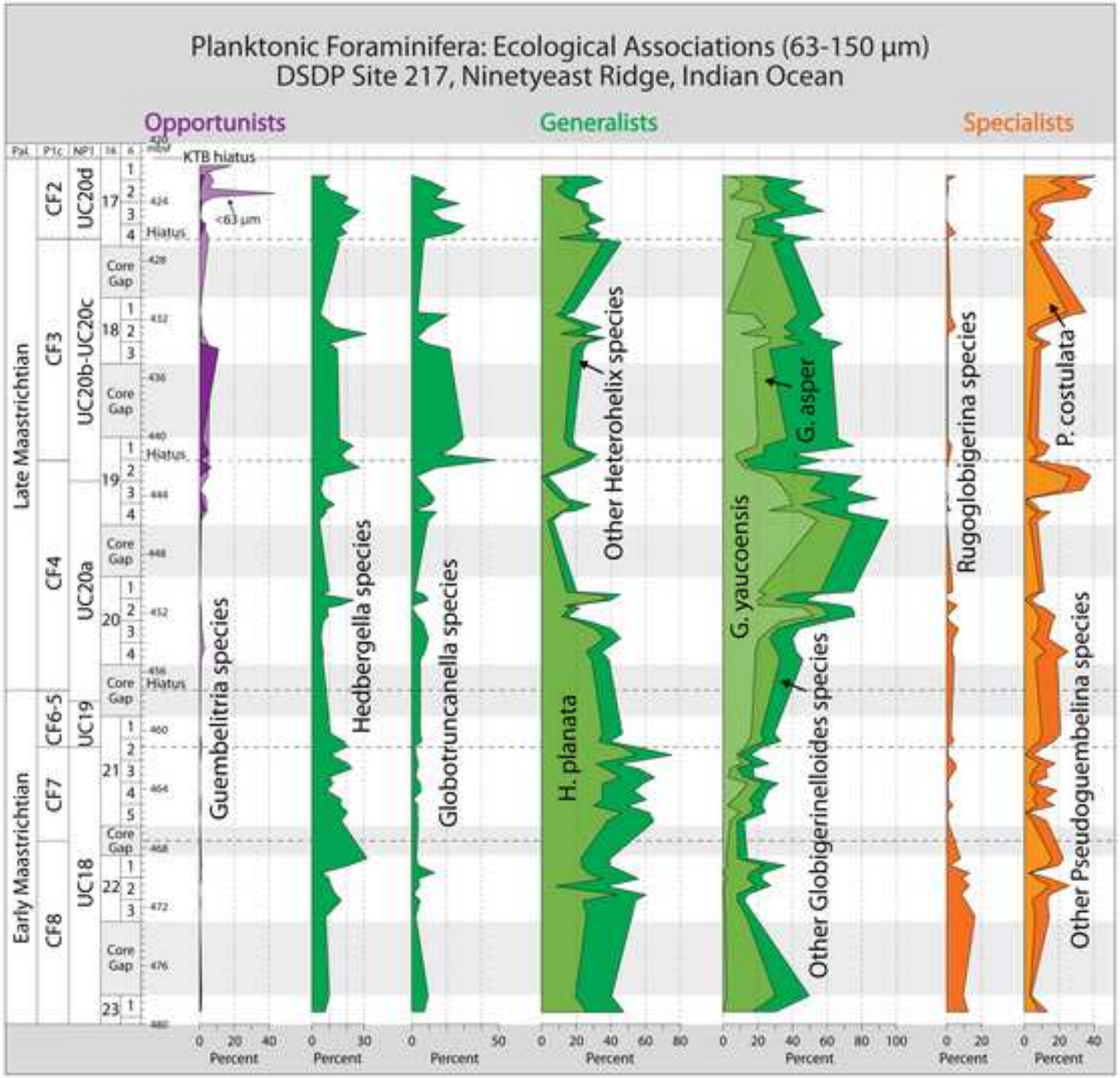

Figure 11

Click here to download high resolution image

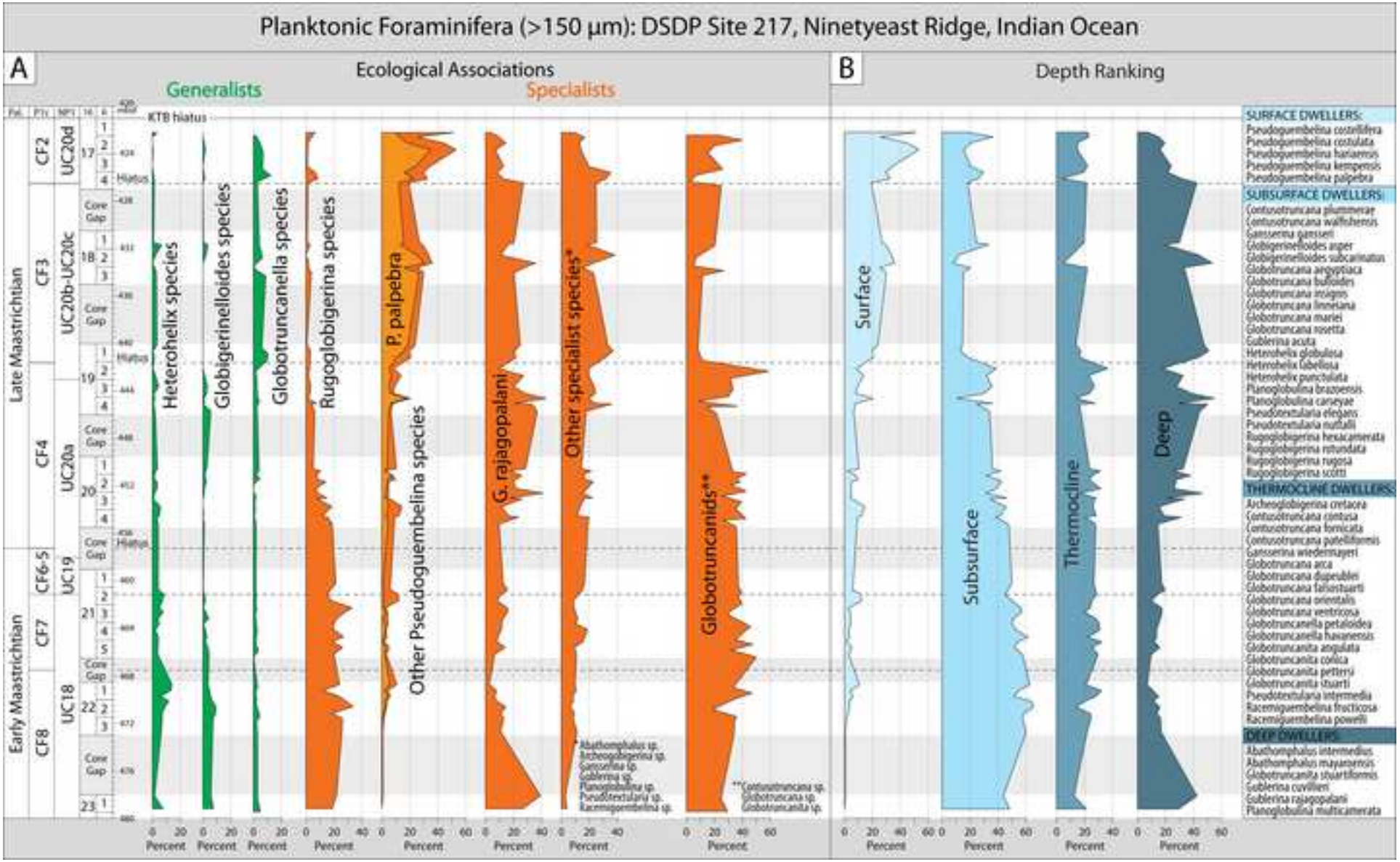

Figure 12

Click here to download high resolution image

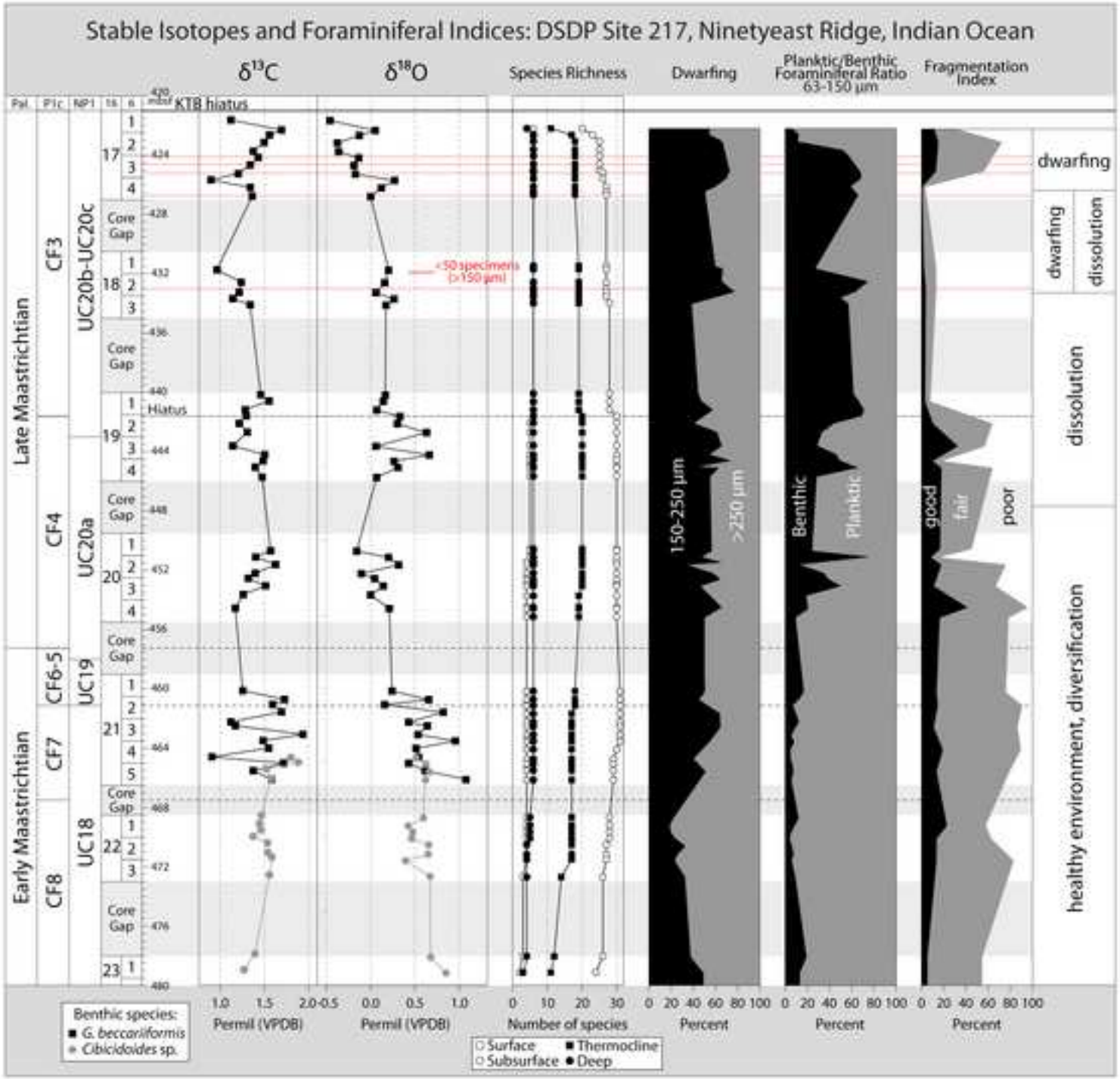

Figure 13

Click here to download high resolution image

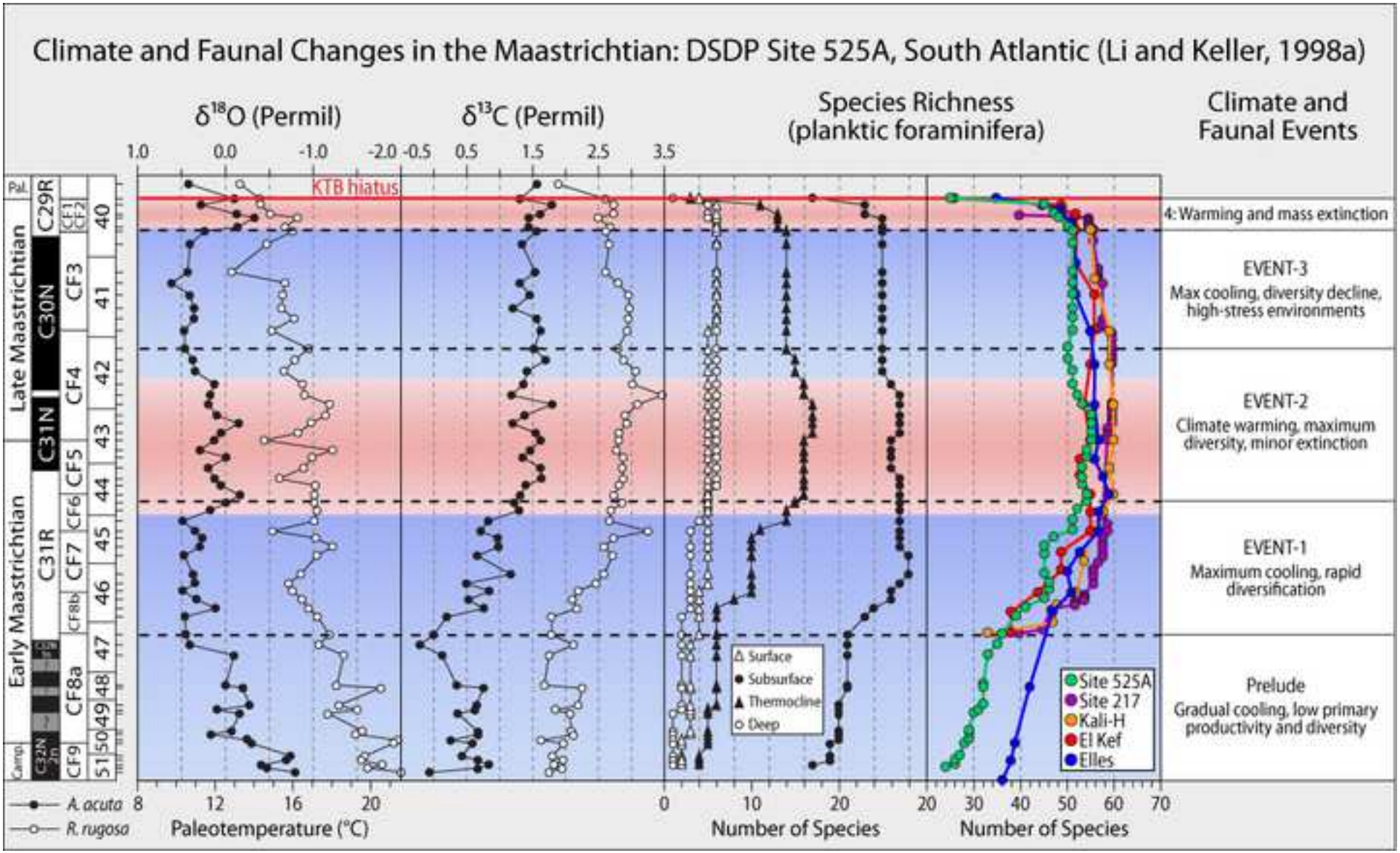

Table 1

Click here to download Table: Table 1.docx

Location	Ninetyeast Ridge	SE India	Tunisia		South Atlantic
	DSDP Site 217	Well Kali-H	El Kef	Elles	DSDP Site 525A
Maximum diversity	60	61	56	59	55
CF8 - N° of species	54	48	42	47	36
CF7 - N° of species	58	54	49	51	45
CF6 - N° of species	59	59	55	58	52
CF5 - N° of species		60	53	58	53
CF4 - N° of species	60	61	55	56	52
CF3 - N° of species	56	56	54	52	51
CF2 - N° of species	54	Hiatus	51	51	49
CF1 - N° of species	Hiatus	Hiatus	49	47	45
N° of species originations Early Maastrichtian Zones CF8b-CF5	14+8*=22	16+9*=25	21	18	23
N° of species originations Early Maastrichtian Zones CF9-CF8a	Not recovered			7	6